Mechanical high-intensity focused ultrasound (histotripsy) in dogs with spontaneously occurring soft tissue sarcomas

Ester Yang

Thesis submitted to the faculty of the Virginia Polytechnic Institute and State University in partial fulfillment of the requirements for the degree of

Master of Science
In
Biomedical and Veterinary Sciences

Shawna Klahn
Nick Dervisis
Eli Vlaisavljevich
Sheryl Coutermarsh-Ott

June 30, 2023
Blacksburg, VA

Keywords: High-intensity focused ultrasound, mechanical ablation, immunotherapy, canine, oncology

Mechanical high-intensity focused ultrasound (histotripsy) in dogs with spontaneously occurring soft tissue sarcomas

Ester Yang

Academic abstract

Background: Histotripsy is a non-thermal, non-invasive high-intensity focused ultrasound (HIFU) ablative technique that causes mechanical fragmentation of tissue, resulting in liquefied acellular debris with histologically clear demarcated boundaries between treated and non-treated tissues. The acellular debris may include tumor antigens with preserved immunogenicity and the potential to generate systemic immune response against tumor cells. Soft tissue sarcomas (STS) are a common form of cancer in dogs with biological behavior similar to STS in humans. Long-term tumor control requires complete removal with extensive surgical resection, which in many cases is not feasible. As a result, there is need for alternative therapies.

Objectives: The primary objective of this study was to demonstrate safety and feasibility of histotripsy in a small animal model of spontaneous STS. The secondary objective was to characterize the impact of histotripsy on the immunologic response.

Materials and methods: Pet dogs diagnosed with spontaneous STS were recruited. CT scan of the chest, abdomen, and the tumor was performed for staging and treatment planning. Pretreatment biopsies were obtained. Safety was monitored with physical examinations, owner reports, and CBC/serum biochemistry. Partial tumor ablation was performed using a 500 kHz prototype histotripsy system. A spherical treatment zone of up to 3 cm diameter in each tumor was treated with histotripsy according to the patient-specific treatment plan using 1-2 cycle pulses applied at a pulse repetition frequency (PRF) of 500 Hz. Anatomical ablation zones were evaluated with contrast CT at 1- and 4-days post-treatment, with tumor resection at 4-6 days

post-treatment. Tumor microenvironment (TME) gene expression was evaluated with the Nanostring Canine IO panel, and the systemic immune response was evaluated using multiplex serum cytokine levels.

Results: Ten dogs were recruited and treated. Tumor histologies included 3 grade III STS, 4 grade II STS, 2 grade I STS, and 1 malignant mesenchymoma. Six dogs were alive, three dogs were euthanized due to disease progression, and one dog was lost to follow up. Histotripsy-related complications were generally self-limiting, with only one patient having increased cutaneous injury score from 1 to 2 (scale 1-5) post-treatment, likely due to prefocal cavitation at the skin. No significant adverse events impacting patient outcome were noted in any of the patients. Visible histotripsy cavitation bubble clouds were seen on real-time ultrasound imaging in nine of ten treatments. Post-treatment histopathology indicated sharply defined regions of ablation that were clearly identifiable grossly and histologically in all samples. Treatment zones were characterized by loss of cell viability, hyalinization, and acute hemorrhage. Post-treatment contrast-enhanced CT images revealed clear, demarcated regions of histotripsy ablated tissue in seven of ten patients.

Differential gene expression analysis identified 79 genes with at least 2-fold change following treatment. Genes associated with inflammation, immune cell migration, and immune cell interactions were the highest upregulated. Amongst the gene set analyses, the myeloid compartment gene sets obtained the highest significance score. There were no statistically significant differences between pre- and post-treatment cytokine concentrations for any of the analytes.

Conclusions: Histotripsy can achieve safe and effective tumor ablation in dogs diagnosed with STS. Histotripsy induced pro-inflammatory changes within the tumor microenvironment.

Histotripsy as an immunotherapeutic treatment option needs to be further investigated.

Histotripsy has a potential to be a precise, non-invasive treatment for canine STS.

Mechanical high-intensity focused ultrasound (histotripsy) in dogs with spontaneously occurring soft tissue sarcomas

Ester Yang

Abstract (public)

Histotripsy is a non-thermal high-intensity focused ultrasound (HIFU) ablative technique that uses controlled acoustic cavitation to cause mechanical fragmentation of tissue. To date, there are no reports investigating histotripsy for the treatment of soft tissue sarcoma (STS). This study aimed to investigate the *in vivo* feasibility of ablating STS with histotripsy and to characterize the impact of partial histotripsy ablation on the acute immunologic response in canine patients with spontaneous STS. CT of the chest, abdomen, and the tumor was performed for staging and treatment-planning. Pretreatment biopsies were obtained. Safety was monitored with physical examinations, through owner reports, and CBC/serum biochemistry. A custom 500 kHz histotripsy system was used to treat ten dogs with naturally occurring STS. Anatomical ablation zones were evaluated with contrast CT at 1- and 4-days post-treatment, with tumor resection at 4-days post-treatment. Safety was determined by monitoring vital signs during treatment and post-treatment physical examinations, routine lab work, and owners' reports. Ablation was characterized using radiologic and histopathologic analyses. Systemic immunological impact was evaluated by measuring changes in cytokine concentrations, and tumor microenvironment changes were evaluated by characterizing changes in infiltration with tumor-associated macrophages (TAMs) and tumor-infiltrating lymphocytes (TILs) using multiplex immunohistochemistry and differential gene expression. Results showed histotripsy ablation can achieve safe and effective tumor ablation in all ten dogs. Immunological results showed histotripsy induced pro-inflammatory changes in the tumor microenvironment. Histotripsy as an immunotherapeutic treatment option needs to be

further investigated. Overall, this study demonstrates histotripsy's potential as a precise, non-invasive treatment for STS.

Acknowledgements

I would like to thank my committee members for their patience and time in helping with this thesis project. Thank you also to the histotripsy engineer team for coordinating the trials.

A big thanks to Dr. Shawna Klahn for her guidance and encouragement throughout my residency. She has helped me with my journey in becoming a research-scientist and a great doctor. Thank you to Dr. Nick Dervisis for his lighthearted nature and words of wisdom on clinics.

Thank you to everyone at ACCRC including my resident mates, the technicians, and previous oncology members, in particular Dr. Keiko Murakami and Dr. Jen Carroll.

Thank you to Dr. Joshua R. White, Esq. for being my person throughout. I am excited to see where life leads us.

A special thanks to my number one cheerleader, my mom. I could not have been a veterinary oncologist without her, and she is the one that made this possible.

Parts of this dissertation i.e., abstracts, chapter 3, and figures have been published in IEEE Transactions on Biomedical Engineering (TBME) and used in the co-authors thesis defense

Chapter 1: Literature Review on Canine Soft Tissue Sarcoma

1.1 Canine soft tissue sarcoma background……. 14

1.1.1: Incidence and Risk Factors……..14

1.1.2: Pathology and Clinical Behavior……14

1.2 Specific Malignant Tumor Subtypes……15

1.2.1: Tumor of Fibrous Tissue……..15

1.2.1.1: Fibrosarcoma (FSA).……15

1.2.1.2: Myxosarcoma……16

1.2.1.3: Pleomorphic Sarcoma……...16

1.2.2: Tumor of the Vascular Wall……17

1.2.2.1: Perivascular wall tumor (PWT)……17

1.2.3: Tumors of Peripheral Nerves……...17

1.2.3.1: Peripheral Nerve Sheath Tumors……..17

1.2.4: Tumors of Adipose Tissue……...18

1.2.4.1: Liposarcoma……..18

1.2.5: Tumors of Skeletal Muscle……..18

1.2.5.1: Rhabdomyosarcoma……..18

1.2.6: Tumors of Lymphatic Tissue……...19

1.2.6.1: Lymphangiosarcoma……19

1.2.7: Tumors of Uncertain Histogenesis……..19

1.2.7.1: Malignant Mesenchymoma……..19

1.3 Diagnostic Technique and Workups……20

1.4 Prognostic and Predictive Factors……21

1.4.1: Histologic Grade……..21

1.4.2: Histologic Subtype……...21

1.4.3: Completeness of Surgical Margins……..22

1.5 Treatment Options……22

1.5.1: Surgery……22

1.5.2: Radiation Therapy……23

1.5.3: Chemotherapy……..24

1.6 Survival……...25

1.7 Conclusion and Translational Applications……25

Chapter 2: Literature Review on High-Intensity Focused Ultrasound

2.1 High-Intensity Focused Ultrasound……27

2.1.1: Thermal High-Intensity Focused Ultrasound……..27

2.1.2: Histotripsy……28

2.2 Immune Modulation from Histotripsy……29

2.3 Conclusion and Translational Applications……30

Chapter 3: Mechanical high-intensity focused ultrasound (histotripsy) in dogs with spontaneously occurring soft tissue sarcomas

3.1 Introduction……..…….32

3.2 Materials and Methods……..…35

3.2.1: Study Population, Screening, and Enrollment Criteria……35

3.2.2: Safety and Feasibility of Histotripsy Treatment……..36

3.2.2.1: Histotripsy system and pressure calibration…….36

3.2.2.2: Histotripsy treatment…….37

3.2.2.3: Evaluation timeline……...38

3.2.2.4: Evaluation of safety and scoring of adverse events……..39

3.2.2.5: Evaluation of ablation effectiveness…….39

3.2.3: Evaluation of Immunological Impact……..40

3.2.3.1: Multiplex immunohistochemistry (mIHC) ……..40

3.2.3.2: Gene expression……41

3.2.3.3: Serum cytokine analysis……...41

3.2.3.4: Statistical Analysis……42

3.3: Results……42

3.3.1: Patient Population……42

3.3.2: Safety and Feasibility of Histotripsy Treatment……..44

3.3.2.1: Adverse event assessment…….44

3.3.2.2: Histotripsy treatment outcomes……45

3.3.2.3: Computed tomography outcomes…….46

3.3.2.4: Gross and histologic findings……...47

3.3.3: Tumor Microenvironment Following Ablation……...47

3.3.3.1: Multiplex immunohistochemistry (mIHC) results……47

3.3.3.2: Gene expression analysis……..48

3.3.4: Systemic Immune Response after Histotripsy……49

3.3.4.1: Serum cytokine analysis……...49

3.4: Discussion……..49

3.5: Conclusion…….55

References

List of Figures

Figures

Figure 1: Experimental histotripsy set-up

Figure 2: Study workflow

Figure 3: Histotripsy treatment feasibility and safety

Figure 4: Representative images demonstrating histotripsy ablation of STS for Patient #5

Figure 5: Multiplex IHC to investigate macrophage populations following histotripsy

Figure 6: Hierarchical clustering of 79 differentially expressed immune-oncology genes

List of Tables

Tables

Tables 1: Patient demographics and tumor characteristics

Table 2: Tumor and ablation zone measurements pre- and post-histotripsy

Table 3: Description and fold changes for top 20 differentially expressed genes

Chapter 1: Literature Review on Canine Soft Tissue Sarcoma

1.1 Canine Soft Tissue Sarcoma Background

1.1.1 Incidence and risk factors

Soft tissue sarcomas (STS) are a common cancer in dogs that arise from mesenchymal tissue with certain unique features based on the cell type of origin. STS comprise of 15% of all skin and subcutaneous tumors in dogs [1]. They are rare tumors in humans, comprising of only 1% of all adult malignancies [2]. Most STS are solitary lesions seen in middle to older-aged large-breed dogs, excluding rhabdomyosarcomas that affect younger-aged dogs, with no breed or sex predilection [1]. The reported annual incidence of canine STS is about 35 per 100,000 of the population at risk [3].

1.1.2 Pathology and clinical behavior

STS is a heterogenous group of tumors of different subtypes classified based on tissue of origin diagnosed on histopathology. Sarcomas are mesenchymal in origin and arise from connective tissue that can produce benign and malignant types of cancers from muscle, adipose, neurovascular, fascial, and fibrous tissue. Thus, STS can develop from a variety of anatomic locations. STS commonly effect the skin and subcutaneous tissues, and most have similar biological behavior. There are also tumor types that arise from soft tissue that are not categorized with the general, umbrella term of STS based on differences regarding anatomic location, biological behavior, and histologic characteristics that exist. These tumors types can include histiocytic sarcomas, rhabdomyosarcoma, peripheral nerve sheath tumor, and hemangiosarcoma, and they all display a higher metastatic rate and commonly are located in visceral locations. Cutaneous and subcutaneous STS are less likely to metastasize and the incidence of local

recurrence is low to moderate following surgical excision, but may be more prevalent depending on grade, subtype, and completeness of excision.

In both dogs and humans, STS are rapidly growing tumors with low metastatic potential, but have the tendency to be locally aggressive. STS slowly grows between fascial planes. But since STS do have the potential to rapidly grow, some tumors have secondary intratumoral hemorrhage and necrosis noted on histopathology. STS often form a pseudocapsule, which is formed by the compression and atrophy of the surrounding tissue as the mass expands, and the expansion of tumor results in a reaction between tumor capsule and normal tissue [4]. The mass can be either firmly fixed or easily moveable to either the underlying skin, subcutaneous space, or musculature. STS can be firm or soft, making them hard to definitively diagnose with just palpation alone.

STS can be further divided into different subtypes depending on the tissue of origin. These subtypes include tumors of fibrous tissues, vascular wall, peripheral nerves, adipose tissue, skeletal muscle, or lymphatic tissue to name a few. Often times STS can be difficult to subclassify as they commonly include collagen matrix and mesenchymal cells forming bundles or whorls. Identifying subtypes may be useful, as some are associated with a higher metastatic rate and unfavorable prognosis.

1.2 Specific Malignant Tumor Subtypes

1.2.1: Tumor of Fibrous Tissue

1.2.1.1: Fibrosarcomas (FSA)

FSA originate from malignant fibroblast that arise on the skin, subcutaneous space, or in the oral cavity. FSA are seen in older-age dogs with no breed or sex predilection. There are few

reports that shows FSA are more prevalent in Golden retriever and Doberman breeds [5]. FSA can range from well-differentiated to anaplastic morphology on histopathology. FSA tend to have higher mitotic rates and are more likely to recur after incomplete surgical excision but more likely to be lower grade [5].

1.2.1.2: Myxosarcoma

Myxosarcomas are derived from fibroblasts with abundant myxoid matrix on the trunk on limbs from the subcutaneous space [6]. However, there are few reports of myxosarcoma arising various parts of the body such as the brain or heart [7,8]. Myxosarcomas are seen in middle-age to older dogs. Myxosarcoms are infiltrative with ill-defined margins and may be associated with higher local recurrence rates and risk of metastasis than other STS. In a recent retrospective study on 32 canine myxosarcoma, there was a high local recurrence of 40.6% and shorter median time to recurrence of around 100 days regardless of other therapy[9]. The metastatic rate to regional lymph nodes and lungs was 25%.

1.2.1.3: Pleomorphic Sarcomas

Pleomorphic sarcomas has histologic characteristics including histocytes and fibroblasts [10]. There is no sex predilection, and these tumors are more prevalent in middle to older aged dogs are. Rottweilers, flat-coated retrievers, and Golden retrievers are overrepresented breeds [11]. Pleomorphic sarcomas are more commonly seen in the subcutaneous tissue, hind limbs, and spleen in dogs. Immunohistochemistry (IHC) staining patterns are not widely used, but these tumors will typically be positive for vimentin and negative for CD18 [12]. There are four histologic subtypes within pleomorphic sarcomas, including storiform-pleomorphic, myxoid, giant cell, and inflammatory. In humans, giant pleomorphic sarcomas have been described as having a higher local recurrence rate and metastatic rate than other subtypes. Giant cell pleomorphic sarcomas

have also been observed to have highly metastatic behavior to the subcutaneous space, lymph nodes, lung, and liver with a median survival time (MST) of only around 60 days in 10 dogs [11].

1.2.2: Tumors of the Vascular Wall

1.2.2.1: Perivascular wall tumors (PWT)

PWT arise from the vascular wall without the endothelial lining[13]. The vascular wall includes different cellular component, and this is dependent on the different kinds of vessel. Capillaries are made up of the basement membrane, endothelium, and pericytes. Great veins and arteries also include subendothelial lining of cells. Broken down these cells include smooth muscle and an adventitial layer of fibroblasts. PWT are defined of high cellularity, capillaries, and spindle cells. PWT have a less aggressive biologic behavior and are unlikely to have local recurrence compared to other histologic subtypes.

1.2.3: Tumors of Peripheral Nerves

1.2.3.1: Peripheral Nerve Sheath Tumors (PNST)

PNST are tumors from Schwann cells which are from nerve sheaths [14]. The most common type of PNST are schwannomas and neurofibromas. These benign tumors are well demarcated and located on the skin or in subcutaneous tissue. Malignant PNST are often cutaneous, ill-defined, and invasive to the deeper tissues and can have poor survivial times due to high rate of local tumor recurrence. Malignant PNST can be differentiated from PWT with IHC staining. Malignant PNST stain as vimentin, glial fibrillary acidic protein, S-100, neuron specific enolase, and nerve growth factor receptor positive [15]. PNST can also affect macroscopic nerves. Plexus PNST can affect the brachial or lumbosacral plexus. In those cases, patients will show signs of limb lameness, muscle wasting, and pain or paralysis [16]. Plexus PNST can invade the

spinal cord and most aggressive treatment options include surgery with adjuvant radiation therapy (RT).

1.2.4: Tumors of Adipose Tissue

1.2.4.1: Liposarcoma

Liposarcomas are derived from lipoblasts and lipocytes with malignant behavior type. Liposarcomas are more commonly seen in older-aged dogs .There is no reported breed or sex predilection [17]. These tumors are usually firm and ill-defined that are usually locally invasive but low metastatic rate. Common primary locations include the ventrum and extremities in the subcutaneous space. Metastatic locations include the lungs and abdominal organs, such as liver and spleen. Liposarcomas can be differentiated from lipomas based on morphologic and cytologic appearance. Liposarcomas are heterogenous and contrast enhancing on pre-contrast CT images. Cytologic staining with Oil Red O can be helpful in diagnosing liposarcomas over other soft tissue sarcomas. The prognosis is usually good when adequate surgical margins are achieved. Following wide surgical excision, the MST is around 3 years [17].

1.2.5: Tumors of Skeletal Muscle

1.2.5.1: Rhabdomyosarcoma

Rhabdomyosarcomas are rare, malignant tumors that originate from myoblasts [18,19]. Rhabdomyosarcomas arise from the skeletal muscle and can be seen in a variety of different places such as the tongue, heart, or bladder. Rhabdomyosarcomas are locally invasive with a low to moderate metastatic rate. Metastatic locations include various locations. The histologic diagnosis of rhabdomyosarcoma can be difficult, and this can be further subclassified as embryonic, botryoid, alveolar, and pleomorphic. IHC staining used to identify rhabdomyosarcomas are positive for vimentin, skeletal muscle actin, myoglobin, myogenin, and

myogenic differentiation (MyoD) [20]. Embryonal rhabdomyosarcoma commonly arises from the anatomical structures above the neck including muscular organs in the oral cavity and eye. Botryoid rhabdomyosarcoma usually are seen in urinary bladders of young female, large breed dogs. This type of cancer have a lower rate of spread compared to the other two types of rhabdomyosarcomas, embryonal and alveolar, which have a higher metastatic rate [18]. Metastatic disease is more commonly seen in younger aged dogs.

1.2.6: Tumors of Lymphatic Tissue

1.2.6.1: Lymphangiosarcoma

Lymphangiosarcoma is a tumor that orignates from lymphatic endothelial cells [21]. Clinical signs are secondary to edema and buildup of lymphatic fluid. Lymphangiosarcomas can be difficult to differentiate from hemangiosarcoma, and IHC markers, such as factor VIII-related antigen and CD31, are used to help guide diagnosis [22].

1.2.7: Tumors of Uncertain Histogenesis

1.2.7.1: Malignant Mesenchymoma

Malignant mesenchymomas are rare STS with limited literature reported on tumor behavior, treatment options, and survival times. Malignant mesenchymoma is composed of two or more different types of sarcoma [23]. These tumors have been reported in various different places and are reported to have a slow rate of growth. However, metastasis has been reported. The survival time and rate for splenic mesenchymomas is better than for dog's with other types of splenic sarcomas [24].

1.3 Diagnostic Technique and Workups

For any mass or nodule of interest, fine needle aspirates for cytologic interpretation are recommended. Because STS do not exfoliate well, a biopsy for histopathology may be needed if cytologies are not successful. The cytologic accuracy can vary and has been reported as low as 63% [25]. In a study looking at the correlation between cytologic features and histologic grade in STS, the number of mitotic figures was the only parameter that showed a significant correlation with grade. Increased number of mitotic figures seen on cytology might correlate with a higher grade. However, the sensitivity of utilizing cytology for grading STS appears to be low and histology should be used to confirm grade [25]. Biopsies should be performed in an area of the tumor where it minimizes surgical dose or size of the radiation field. A biopsy can give more information about the STS than cytology samples such as the grade and subtype. However, it should also be interpreted with caution. Histologic grade from preoperative biopsies showed a discordance in interpretation in 41% of dogs compared with surgical samples. Of those that lacked concordance, 29% of pretreatment biopsies underestimated the grade. Excisional biopsies are not recommended and can cause more morbidity from an aggressive surgery or multiple attempts at resection.

Diagnostic tests such as routine bloodwork and chest radiographs are recommended prior to anesthesia for any middle-aged to older dogs. Although metastasis is uncommon, full staging would include abdominal imaging to assess for tumor spread into abdominal organs. Imaging can also include CT or MRI for staging and surgical planning if the mass is large, firmly fixed, or in locations that may not be easily accessible for surgery.

1.4 Prognostic and Predictive Factors

Several factors for STS are important influencers of prognosis including histology grade, subtype, and completeness of surgical margins. Other potential features include tumor size, invasiveness, location, and stage. Knowing this information helps to formulate treatment goals and options for our patients.

1.4.1: Histologic Grade

Histologic grade was developed to take into account the degree of differentiation, mitotic index, and necrosis of a tumor. Grade also helps to give us invaluable prognostic information on recurrence and metastasis. Grade I tumors have the lowest likelihood to recur following excision. In one study, histologic grade III STS had around a six-fold increased risk for local recurrence when compared to grade I. When surgical margins are close, grade I tumors recur at an infrequent rate of 7% [26]. Similarly, metastasis of grade I tumors are rare and reported at a rate of 7-13% [27]. Grade III tumors have the greatest potential for recurrence and metastasis. Grade III STS with close margins can recur up to 75%, and reports of metastatic rate for grade III STS have been reported up to 44% [4]. As such, grade is a useful prognostic indicator in terms of predicting recurrence and having concern for metastasis. Prevalence of pulmonary nodules is about 11.7% in a study with likelihood higher for dogs with grade III STS and for dogs with STS having been present for greater than three months.

1.4.2: Histologic Subtype

Histologic subtype may also contribute to local tumor recurrence. Certain subtypes such as fibrosarcoma have been associated with higher local tumor recurrence compared to perivascular wall tumor subtypes. Tumor size also has been associated with a negative effect on local tumor control. Recurrence is greater than 5-fold in PWTs larger than 5-cm in diameter

treated with marginal resection. Dogs with fixed or invasive STS have significantly decreased disease free interval (DFI) and MST as well [28].

1.4.3: Completeness of Surgical Margins

The body of most solid tumors is usually necrotic or hypoxic, whereas the leading edge or legs of the tumor can be more invasive and well vascularized. Thus, the width of lateral margins includes beyond the pseudocapsule and is dependent on the tumor type. To decrease risk of local tumor recurrence, curative intent surgeries usually include wide excision. Wide excision of STS attempts to obtain 3-cm laterally from the edge of the tumor and one fascial plane deep. Radical excision can also be an option and usually requires amputation dependent on the anatomic location of the mass. Completeness of surgical margins is a major factor for recurrence, and it is significantly more likely achieved with wide resection compared to more conservative approaches [5]. STS with complete margins is less likely to recur. Local tumor recurrence has been associated with increased risk of tumor related death and decreased survival times [29].

1.5 Treatment Options

The goal and challenge for managing STS is local tumor control. Thus, the treatment of choice is surgical resection. Radiation therapy (RT) may also be a treatment option, especially for incompletely excised tumors. The treatment plan is tailored after physical examination, staging, histologic grade, and the client's goals.

1.5.1: Surgery

Surgical options include marginal, wide, and radical resection. The surgical approach is based on multifactorial reasons such as tumor location, size, grade, and the client's goals. STS are characterized as a locally expanding mass that can be infiltrative to the underlying

musculature as well. In a study evaluating neoplastic infiltration of the skin, about 36% of dogs were reported to show cutaneous infiltration even in grade I tumors. Not surprisingly, there was higher frequency of infiltration that was observed with higher grades [30]. STS have a pseudocapsule that can give observers a false impression of the tumor being well encapsulated and could lead to incomplete surgical resection. Regardless of subjective appearance, the recommended margins for wide surgical resection are 3-cm lateral margins with 1-fascial layer deep to the tumor. Radical surgery usually includes limb amputation to achieve adequate local tumor control for fixed and invasive STS on the limb. Wide surgical excision is associated with increased likelihood of complete excision compared to marginal excision. Marginal excision is an option for well-circumscribed, non-infiltrative STS smaller than 5-cm in diameter. Local tumor recurrence was more likely to occur with fixed and invasive STS as they can lead to inadequate options margins. Treatment options for incompletely excised STS include active surveillance, re-surgical excision, radiation therapy, or chemotherapy depending on grade [5,29]. In one study evaluating dogs with subcutaneous STS, the local recurrence rate was 0% when the tumor was completely excised. The local recurrence rate increased for incompletely excised high-grade tumors. For incompletely excised grade I, grade II, and grade III STS, there was a 7%, 35%, and 75% risk of developing recurrence respectively[26].

1.5.2: Radiation Therapy

Canine STS have a biological behavior similar to that of low-grade STS in people and RT improves local tumor control in people with incompletely excised STS. RT is also utilized to manage incompletely excised canine STS. Local tumor control for incompletely excised STS with adjunctive definitively fractionated RT is good with reported 1-, 2-, and 3- year local tumor control rates of 71-84%, 60-81%, and 57-81% respectively [31-33]. In a study using definitive intent

radiation therapy in 41 dogs with incompletely excised high-grade STS, the overall survival time (OST) was 981 days. During this time 24% and 20% developed metastasis and local recurrence, respectively. Chemotherapy did not improve outcomes in dogs. The hazard of death over the study period increased when RT duration was long [34]. In 35 dogs treated with curative intent stereotactic body radiant therapy (SBRT), the time to tumor progression (TTP) and OST was 705 days and 713 days, respectively. Low histologic grade and locations on the extremity were positive prognostic factors on survival time. Radiation therapy was overall well tolerated and acute side effects were limited to the skin [35]. There have also been cases RT was used for macroscopic canine STS. In a retrospective study of 50 cases treated with 5 x 6 Gy protocol in macroscopic tumors, the median progression free interval (PFI) for all cases was around 400 days and OST of around 500 days. Dogs with tumors on the limb had longer PFI and OST. The addition of metronomic chemotherapy yielded a longer OST compared to no systemic treatment, but it does not influence PFI. Toxicity was low during treatments.

1.5.3: Chemotherapy

The role of chemotherapy in controlling canine STS is generally unknown. Overall, the consensus is that adjuvant chemotherapy is not effective in local tumor control [36]. However, the one study that looked into metronomic cyclophosphamide therapy with piroxicam on tumor recurrence in incompletely resected STS showed DFI was prolonged in treated dogs compared with untreated controls [37]. There may also be a role for chemotherapy in grade III STS to theoretically decrease the metastatic rate.

1.6 Survival

The overall MST ranges from 1,013 to 1,796 days after surgery alone [28]. This number can change depending on specific soft tissue sarcoma subtypes. Additionally, dogs with grossly invasive and fixed STS have a 5-fold increased risk of tumor death. The MST is good in dogs treated wide surgical margins and is reported to be greater than 1,000 days.. This is significantly greater than dogs treated with non-curative intent surgeries of 264 days [5]. Many clinical factors need to be taken into account regarding survival times.

1.7 Conclusion and Translational Applications

STS are rapidly growing tumors with low metastatic potential, but locally aggressive behavior. The complexity of the tumor is characterized by its variable presentation and behavior, and treatment typically requires a multimodal approach for incompletely excised or hard to access tumors. Adequate local tumor control requires surgical resection of tumor if the tumor is small and accessible, or a combination of surgery and radiation therapy to address microscopic disease to reduce the risk of recurrence. As a result, novel techniques are still needed to treat soft tissue sarcoma to address all types of tumor scenarios.

Spontaneous tumors in dogs are becoming a translational bridge between veterinary and human oncology research [38-41]. Naturally occurring cancers in animals act as a cancer research model to address treatment challenges and tumor biology questions through their tumor heterogeneity. Soft tissue sarcomas are much less common in humans, but the biological behavior is similar in both species. Similar to humans, grade and stage are prognostic in dogs. Most tumors were diagnosed as the human equivalent of undifferentiated sarcoma, spindle cell sarcoma, or unclassified spindle cell sarcoma [3]. There is need for alternative local therapies, and

immunotherapy is an attractive option to address the microscopic disease. Canine STS as a translational model provides an opportunity to advance medical knowledge and therapies for a human disease for which the low tumor incidence can make recruitment in human patients challenging. It also opens up the possibility on how to change the tumor microenvironment of an immunogenically quiet tumor as there are no reports of immune cell infiltration into the tumor. High-intensity focused ultrasound has the capability to address both the local and systemic needs for many types of tumors, including STS.

Chapter 2: Literature Review on High-Intensity Focused Ultrasound

2.1 High Intensity Focused Ultrasound

High-intensity focused ultrasound (HIFU) is an ablation technique able to destroy tissue by either thermal or mechanical means [42]. Within the umbrella term of HIFU, two main modalities exist: thermal HIFU and mechanical HIFU, or alternatively known as histotripsy. Our research team has utilized both in the treatment for canine and feline soft tissue sarcomas.

2.1.1 Thermal High-Intensity Focused Ultrasound

Thermal HIFU effect is achieved through the absorption of ultrasound energy from a continuous wave HIFU pulse for a couple of seconds and can elevate the temperature in the local tissue that can last for minutes [43]. This temperature elevation results in thermal coagulation which can cause protein denaturation and irreversible cell damage[44]. The ultrasound pulse is focused within a small volume of treatment area to minimize potential for thermal diffusion and secondary thermal injury to the surrounding tissues. The immunostimulatory effects of HIFU may be related to its ability to promote immunogenic cell death. The in-situ tumor debris remaining after thermal ablation will contain tumor antigens [45]. The tumor antigens present can either passively enter circulation or be recognized by an antigen presenting cell in order to present them to immune effector cells to initiate adaptive antitumor immune response. The preserved tumor antigens could essentially function as an in-situ cancer vaccine able to stimulate local and even distant systemic immune responses for an abscopal effect [46]. Thus, thermal HIFU is a less invasive and potentially immunogenic alternative to standard local treatment options. To date, our team has treated 15 dogs with peripheral STS, demonstrating thermal HIFU treatment to safely achieve complete tumor kill in the ablation zone[47]. A survival analysis on the 18 dogs

that were treated according to protocol was performed and a median survival time (MST) was not reached. When censoring the fifteen dogs that were still alive at the time of data analysis, a MST of 334 days were calculated. Histologically, there was a clear demarcation between treated tissue and non-treated tissue. There was a subjective increase in CD3+ immune cells along the zone of transition and within the ablation zone. Additionally, there was a >2-fold increase in multiple genes associated with pro-inflammatory cytokine signaling in post-treatment samples indicating an inflammatory response in the TME. These preliminary results in our first in-patient trial of canine solid tumors found HIFU to be safe, feasible, and cause predictable ablation. This opened the door to investigate the newer HIFU modality, histotripsy.

2.1.2 Histotripsy

While traditional HIFU relies on the absorption of ultrasound energy to thermally destroy tissue, histotripsy is a non-thermal technique that uses repeated short pulses of ultrasound waves to mechanically disintegrate tissue into a liquefied acellular debris [48-51]. Histotripsy is applied in short cycles of high pressure pulses to produce inertial cavitation bubbles, which form a precise histotripsy bubble cloud at the targeted location within the tissue [52,53]. The human body has small nanometer endogenous gas pockets that are stabilized with high surface tensions. Using histotripsy, we can raise the pressure outside of the gas pocket high enough to overcome surface tension. This will make the gas pocket grow in size and form microbubbles in the tissue of interest. Using just a single ultrasonic pulse, we can exceed the intrinsic cavitation threshold, or the threshold at which microbubbles appear, of that tissue to reliably generate a single bubble cavitation. Within 3-4 cycles, a large bubble cloud can form. The quick growth and breakdown of these bubbles causes mechanical disruption of the cellular structure resulting in emulsified acellular debris that can be absorbed as part of the body's physiologic healing process [50,54].

Through bubble cavitation, histotripsy results in localized tissue removal with sharp boundaries. Histotripsy treatment is typically guided in real-time by ultrasound imaging, allowing the precise and non-invasive targeting of tissues.

The inherent intrinsic stiffness of the tissue is strongly correlated with the cavitation threshold. Fibroblast have a higher cavitation threshold compared to squamous cell carcinoma. Following histotripsy of the kidney, there is more damage in the cortex compared to the medullary tissue since the medulla contains more fibrous connective tissue [55]. This has also been reported in prostatic tissue where the urethra is stiffer than the prostate and more acoustic pulses are needed to preferentially ablate the urethral tissue [56]. Knowing the intrinsic stiffness of the tissue can be advantageous as the user can choose optimal histotripsy settings to destroy one type of tissue and salvage another, such as blood vessels, within the treatment zone.

2.2 Immune Modulation from Histotripsy

In addition to its ablative potential, histotripsy may also promote immunostimulatory effects related to its ability to induce immunogenic cell death [57]. Studies of HIFU in rodent tumor models have demonstrated that HIFU is immunogenic and that histotripsy may result in more robust immune responses than thermal HIFU [45,46,58]. The in-situ tumor debris remaining after mechanical ablation may include tumor neoantigens in their native form, preserving immunogenicity and the potential to generate a systemic immune response against tumor cells. These tumor neoantigens can be recognized by antigen presenting cells, activating immune effector cells and initiating immune cell infiltration. The resulting antitumor immune response may then stimulate local and systemic immune responses [58]. Early studies investigating these

effects have reported that histotripsy treatment in a murine cancer model can alter the tumor microenvironment and activate the immune response [46,57-62].

Rodent xenograft and *in vitro* studies have demonstrated that HIFU is immunogenic, and studies report a more robust immune response and decreased rate of metastasis following histotripsy compared to thermal HIFU. In a recent study, histotripsy ablation of subcutaneous melanoma tumors resulted in a significant increase of intratumoral CD8+ T cell infiltration in mice compared to radiation or thermal ablation therapy [63]. The immunostimulatory effects of thermal ablation may be related through heat-based denaturation and necrosis. In contrast, histotripsy exerts its immunostimulatory effects through its ability to promote immunogenic cell death. Histotripsy instigates cell membrane disruption while preserving subcellular components that could have immunogenic effects on tumors cells. The nonviable tumor debris created by histotripsy still contains peptide tumor antigens with preserved immunogenicity. A two-tumor model in this study demonstrates that single histotripsy tumor ablation is capable of stimulating abscopal CD8+ tumor infiltration response seen by diffusely localized T-cell infiltrates at distant tumor sites [58]. The abscopal effect is shown by inhibiting distant pulmonary metastases.

2.3 Conclusion and Translational Applications

Previous preclinical studies have shown that histotripsy can ablate various distinct tumor types including prostatic [64], intracranial [65], pancreatic [59], and hepatic tumors [66,67]. Histotripsy has yet to be investigated in canine soft tissue sarcomas.

A study investigating the effectiveness and safety profile of histotripsy in human patients with primary and secondary liver tumors was able to achieve a defined tissue destruction zone in a predictable manner. There was no treatment associated adverse events reported, and this first

in human trial demonstrated that histotripsy is effective in destroying liver tissue predictably and safely[68]. Our group has also recently explored the use of histotripsy in feline soft-tissue sarcomas. Results of this study showed that histotripsy was able to target and ablate superficial feline soft tissue sarcomas. Further use of histotripsy in veterinary medicine could be a viable option and future studies will help to guide clinical application in one-health medicine[69].

Currently, only local tumors of considerable size can be treated and not distant micro-metastases. The immunologic effects of HIFU need to be further investigated. Canine STS create a unique opportunity as we take an immunogenically cold tumor and assess the dog's immune responses following treatment.

Chapter 3: Mechanical high-intensity focused ultrasound (histotripsy) in dogs with spontaneously occurring soft tissue sarcoma

Lauren Ruger and Ester Yang contributed equally to this work and this manuscript was accepted for publication in IEEE. Transaction on Biomedical Engineering (TBME) on August 21, 2022 (DOI: 10.1109/TBME.2022.3201709).

Authors: Lauren Ruger, Ester Yang, Jessica Gannon, Hannah Sheppard, Sheryl Coutermarsh-Ott, Timothy J. Ziemlewicz, Nikolaos Dervisis, Irving C. Allen, Gregory B. Daniel, Joanne Tuohy, Eli Vlaisavljevich, Shawna Klahn

3.1 Introduction

High-intensity focused ultrasound (HIFU) is a non-invasive ablation technique with the ability to destroy tissue by thermal or mechanical means. While traditional HIFU relies on the absorption of ultrasound energy to thermally destroy tissue, histotripsy is a non-thermal technique that uses repeated short pulses of ultrasound waves to mechanically disintegrate tissue into a liquefied acellular debris [48-51]. Histotripsy applies short (1-10 cycles), high pressure (>15-30 MPa) pulses to produce inertial cavitation, which form a precise histotripsy bubble cloud at the targeted location within the tissue [52,53]. The subsequent rapid expansion and collapse of these bubbles causes mechanical disruption of the cellular structure, reducing treated tissues to emulsified acellular debris that can be absorbed as part of the body's physiologic healing process [50,54]. Histotripsy treatment is typically guided in real-time by ultrasound imaging, allowing the precise, non-invasive targeting of tissues ranging from deep, visceral structures to superficial, subcutaneous tumors. Previous preclinical studies have shown that histotripsy can successfully ablate various tumor types *ex vivo* and *in vivo*, including prostate [64], kidney [61], bone [70], brain [65], pancreatic [59], and liver tumors [66,67]. Additionally, a recent human clinical trial has shown safe and effective ablation of primary and metastatic liver tumors [60]. The results of these prior studies suggest that histotripsy has the potential to be a paradigm-shifting method for image-guided,

non-invasive tumor ablation. While widely explored for other tumor types, histotripsy not yet been explored for the ablation of superficial soft tissue sarcoma tumors.

In addition to its ablative potential, histotripsy may also promote immunostimulatory effects related to its ability to induce immunogenic cell death [57]. Studies of HIFU in rodent tumor models have demonstrated that HIFU is immunogenic and that histotripsy may result in more robust immune responses than thermal HIFU [45,46,58]. The *in situ* tumor debris remaining after mechanical ablation may include tumor neoantigens in their native form, preserving immunogenicity and the potential to generate a systemic immune response against tumor cells. These tumor neoantigens can be recognized by antigen presenting cells, activating immune effector cells and initiating immune cell infiltration. The resulting antitumor immune response may then stimulate local and systemic immune responses [58]. Early studies investigating these effects have reported that histotripsy treatment in a murine cancer model can alter the tumor microenvironment and activate the immune response [46,57-62]. Similarly, a case of an abscopal effect was identified in the human clinical trial investigating histotripsy for liver tumor ablation [71]. These findings, combined with prior work showing that thermal HIFU can target and treat STS tumors in both dogs [72,73] and humans [74-76], have led our team to initiate this study to investigate histotripsy's ablative and immunological effects for treating STS in pet dogs as a clinical model [70,77].

Spontaneous tumors in pet dogs are increasingly recognized for their value in translational oncology research [38-41]. Naturally arising cancers in dogs provide a cancer research model to address pre-clinical questions and challenges through their genetic diversity, tumor heterogeneity, and by following similar biological and therapeutic courses as their human counterparts. Canine cancers arise naturally within the complex interactions between the tumor,

the tumor microenvironment, and the host immune system, providing a unique opportunity to evaluate and refine immunotherapy strategies [78-81]. Soft tissue sarcomas (STS) are a common cancer in dogs and arise from mesenchymal tissues, representing different types of tumors with similar histologic features and biologic behavior. STS compromise of 15% of all skin and subcutaneous tumors in dogs, but are rare tumors in humans, comprising only 1% of all adult malignancies [2,82]. Canine STS as a translational model provides an opportunity to advance medical knowledge and therapies for a human disease for which the low tumor incidence can make recruitment of sufficient human patients challenging. STS are rapidly growing tumors with low metastatic potential, but locally aggressive behavior. The complexity of the tumor is characterized by its variable presentation and behavior, and treatment typically requires a multimodal approach. Adequate local tumor control requires either complete removal of the tumor with extensive surgical resection of adjacent grossly normal tissue or a combination of surgery and radiation therapy to address microscopic disease, reducing the risk of recurrence. As a result, novel techniques are still needed to treat soft tissue sarcoma while preserving adjacent healthy tissue.

The objective of this study was to demonstrate the *in vivo* safety and feasibility of ablating soft tissue sarcomas with histotripsy in canine patients with spontaneous STS. Our secondary objective was to characterize the impact of the histotripsy ablation on the acute immunologic response in the tumor microenvironment. A custom 500 kHz histotripsy system was used to treat ten client-owned dogs with soft tissue sarcomas in order to test whether histotripsy could achieve safe and effective ablation of targeted tumor regions in dogs with naturally occurring STS tumors. Four to six days after histotripsy treatment, tumors were surgically resected. Radiologic (i.e., CT) and histopathology assessments were conducted to

determine (1) the efficacy of the histotripsy ablation and (2) the impact of a single histotripsy treatment within a portion of the STS on the immunologic response.

3.2 Materials and Methods

3.2.1: Study Population, Screening, and Enrollment Criteria

This was a prospective, single-arm, open-label pilot study of histotripsy treatment in dogs with soft tissue sarcomas. Client-owned dogs with naturally occurring tumors presented to the Animal Cancer Care and Research Center (ACCRC) over an 8-month period (September 2, 2020 - May 10, 2021) were recruited for enrollment. The owners of eligible dogs were offered standard treatment options, including palliative care. Informed consent was obtained for all enrolled dogs. This study was approved by the University Institutional Animal Care and Use Committee (#20-049) and the College of Veterinary Medicine Hospital Board.

Canine patients with cytologic or histological diagnosis of a peripheral, malignant soft tissue tumor were considered for enrollment. Tumor-specific inclusion criteria were a diameter of at least ≥ 2 cm; an accessible solid area for treatment; and, surgically resectable, as determined by an ACVS-board-certified surgeon who is a surgical oncology fellow. Patients were required to undergo routine laboratory bloodwork, and thoracic and abdominal imaging at screening. The patient had to have an expected survival time of >6 weeks without treatment. Patients were excluded if the tumor was non-resectable or if the recommended surgical resection was declined, if the patient had definitive therapy other than surgery within the past 3 weeks, or if a co-morbidity precluded anesthesia: significant cardiac dysfunction, creatinine value >1.2x the upper reference limit (URL), ALT or AST values >3.0x the URL, or total bilirubin value >1.2x URL.

3.2.2: Safety and Feasibility of Histotripsy Treatment

3.2.2.1: Histotripsy system and pressure calibration

The array transducer was built in-house using rapid prototyping technology and was integrated onto a prototype clinical histotripsy system (HistoSonics, Ann Arbor, MI, USA) before treatment [**Fig. 1**]. After aligning the imaging probe coaxially within the therapy transducer, the transducer assembly was attached to a triaxial robotic micro-positioner mounted on the clinical system via an articulating arm. The transducer was driven using a custom high-voltage pulser designed to generate single cycle therapy pulses of controlled by a preprogrammed field-programmable gate array (FPGA) board (Altera DE0-Nano Terasic Technology, Dover, DE, USA). The transducer was powered by a high voltage DC power supply (GENH750W, TDK-Lambda, National City, CA, USA) and controlled by a custom MATLAB script (The MathWorks, Natick, MA, USA) written to receive a trigger from the clinical system. Before treatment, focal pressure waveforms for the 500 kHz transducer were measured using a high-sensitivity reference rod hydrophone (HNR-0500, Onda Corp., Sunnyvale, CA, USA) and a cross-calibrated custom-built fiber optic hydrophone (FOPH) in degassed water at the transducer's focal point [83,84]. The rod hydrophone was also used to measure the lateral, elevational, and axial 1-D focal beam profiles of the transducer by scanning the hydrophone incrementally over a distance wider than the focal width at a peak negative pressure (*p-)* of ~1.8 MPa. The measured transverse, elevational, and axial full-width half-maximum (FWHM) dimensions at the geometric transducer were measured to be 2.1 mm, 2.1 mm, and 6.6 mm, respectively. Focal pressures were measured directly with the FOPH up to a peak negative pressure of ~20 MPa; at peak negative pressures greater than ~20 MPa, the focal pressure was estimated by summing measurements from a subset of a quarter and a half of the total elements

to prevent cavitation from forming on the fiber. All waveforms were measured using a Tektronix TBS2000 series oscilloscope at a sample rate of 500MS/s; then, the waveform data was averaged over 128 pulses and recorded in MATLAB.

3.2.2.2: Histotripsy treatment

Patient-specific treatment plans were developed using pre-treatment CT images, physical examinations, and freehand ultrasound imaging. Patients were anesthetized following standard protocols for client-owned dogs. Anesthesia was maintained using inhaled isoflurane, and anesthesia parameters were measured every five minutes (blood pressure, pulse, and ventilation) or every fifteen minutes (oxygen saturation, carbon dioxide saturation, body temperature, and cardiac arrhythmias). The treatment area was clipped and closely shaved using a razor to remove overlying fur. The histotripsy transducer was positioned over the treatment site and placed in a container of degassed water (<30% dissolved O_2) coupled to the canine patient to ensure acoustic propagation from the transducer to the skin. Fine adjustments to correctly position the transducer over the targeted region were made using the robotic micro-positioner.

Each tumor was treated with histotripsy according to the patient-specific treatment plan using one cycle pulses applied at a pulse repetition frequency (PRF) of 500 Hz. Prior to the volumetric treatment, the pressure at the focus was increased incrementally until a visible bubble cloud was generated on ultrasound imaging. A spherical treatment volume fully contained within the tumor was set manually within the software of the system. After identifying a pressure level for treatment and setting the treatment boundaries, an automated volumetric histotripsy was applied to a 3D grid of equidistant treatment points within the defined boundaries. Treatment points were spaced by 3.5 mm in the axial direction and 1.5 mm in the lateral and elevational directions to allow overlap between the bubble cloud at each location. The robotic micro-

positioner moved the focus between treatment locations, and each point was treated with ~500 pulses. The histotripsy treatment parameters employed in this study were chosen based on previous histotripsy studies for other soft tissue applications [59,67,85,86]. The bubble cloud and tissue effects were monitored during treatment using real-time ultrasound imaging. The histotripsy treatment workflow is summarized in **Fig. 2**.

3.2.2.3: Evaluation timeline

Within 10 days prior to treatment, baseline evaluation included an examination; Complete Blood Count (CBC) and serum biochemistry; tumor measurements using calipers and gross photographs; contrast CT scan (SOMATOM Confidence® RT) of the thorax, abdomen, and tumor; and pre-treatment biopsy. The pre-treatment biopsy was performed outside of the planned treatment zone. On the day of histotripsy treatment, an exam and tumor photographs were obtained immediately prior to, during, and immediately following treatment. One day post-treatment, an exam, CBC, serum biochemistry, tumor measurements and photographs, and contrast CT scan of the tumor were performed. Four to six days post-treatment, tumor measurements and photographs, CBC, serum biochemistry, and contrast CT scan of the tumor were performed immediately prior to surgical resection. Surgical excision and post-operative recommendations for all canine patients were directly performed or supervised by an oncology-fellowship-trained Diplomate of the American College of Veterinary Surgeons (ACVS). Patients were examined and the surgery site was photographed two weeks after surgery. Post-study monitoring recommendations were at clinician discretion, including monthly physical exams and thoracic radiographs appropriate to the patient's tumor type and stage. Patient outcome was documented by communication with the owner or primary-care veterinarian.

3.2.2.4: Evaluation of safety and scoring of adverse events

Safety was monitored with physical examinations, owner-reported outcomes, CBC, and serum biochemistry profiles. Adverse events (AEs) were graded according to the Veterinary Cooperative Oncology Group-Common Terminology Criteria for Adverse Events (VCOG-CTCAE v1.1) [87]. Severe adverse events (SAEs) were defined as any grade 4/5 toxicity.

3.2.2.5: Evaluation of ablation effectiveness

Tumor ablation was evaluated for targeting feasibility and ablation completeness through a combination of ultrasound imaging, contrast-enhanced CT images, and gross and microscopic tissue evaluation. Ultrasound imaging was used to confirm the formation of the histotripsy bubble cloud during histotripsy treatment and to monitor for echogenicity changes in the treated tissues after ablation. Contrast CT scans were performed at three timepoints (baseline, one day post-treatment, and four to six days post-treatment) and analyzed to determine changes in overall tumor volume post-treatment and to measure ablated tissue volumes. All CT measurements were completed by a trained radiologist blinded to planned histotripsy treatment volumes (T.J.Z.). Differences between pre- and post-treatment tumor volumes as well as differences between 1 day post- and 4 day-post treatment ablation zone dimensions were compared using two-tailed and one-tailed paired student's t-tests, respectively. Immediately following surgical removal, the tumor was sectioned and gross photographs were obtained identifying the ablation zone. Representative sections of the pre-treatment tumor, treated tumor, treatment interface, and untreated tumor were fixed in 10% formalin for at least 24 hours and embedded in paraffin. A standard hematoxylin and eosin (H&E) stain was used to stain all tissues to assess the extent of histotripsy damage to the tissue. All sections were evaluated by a veterinary pathologist and Diplomate of the American

College of Veterinary Pathologists (ACVP) with extensive experience evaluating ablated tumor tissue (S.C.O.).

3.2.3: Evaluation of the Immunological Impact

3.3.2.1: Multiplex immunohistochemistry (mIHC)

Optimized chromogenic multiplex immunohistochemistry (IHC) was performed on formalin-fixed, paraffin-embedded (FFPE) samples in order to investigate the presence and phenotype of infiltrating immune cells following histotripsy treatment. Two multiplex IHC panels were applied to treated and untreated tumor samples from the same patient and then compared. Tumor-associated macrophages (TAMs) and tumor-infiltrating lymphocytes (TILs) were investigated. The Roche Ventana Discovery Ultra Automated Research Stainer (Roche Diagnostics, Indianapolis, IN) was used according to the manufacturer's instructions for IHC multiplexing. To characterize TAMs, tissues were stained with antibodies against pan-macrophage marker IBA-1 (FujiFilm, 019-19741, 1:300), M1-polarization marker iNOS (Abcam, ab3523, 1:100), and M2-polarization marker CD206 (NovusBio, NBP190020, 1:200). To characterize TILs, tissues were stained with antibodies against pan T-cell marker CD3 (DAKO, A0452, 1:100), helper T-cell marker CD4 (Origene, TA500477, 1:100), cytotoxic T-cell marker CD8 (Invitrogen, PAS-16893, 1:100), and regulatory T-cell marker FOXP3 (Invitrogen, 14-7979-82, 1:100). Signals were generated using the following chromagens: IBA-1 and CD4, purple; iNOS and CD8, teal; CD206 and CD3, yellow; and FOXP3, DAB (Roche Diagnostics, Indianapolis, IN). Multiplex-stained slides were imaged at 20X or 40X magnification using the Vectra® Polaris™ Automated Quantitative Pathology Imaging System (Akoya Biosciences, Marlborough, MA) and evaluated by a veterinary pathologist and Diplomate of the American College of Veterinary Pathologists (ACVP) (S.C.O.).

3.2.3.2: Gene expression

Tumor microenvironment gene expression was evaluated with the NanoString Canine IO panel (XT-CIO-12, NanoString, Seattle, WA). RNA was extracted using the RNeasy FFPE kit (Research Products International Quick-RNA FFPE MiniPrep, RPI-ZR1008) following manufacturer instructions. Pre-treatment RNA was extracted from formalin-fixed paraffin-embedded (FFPE) soft tissue tumor scrolls of sections of pre-treatment samples, or from untreated tumor if pre-treatment samples were inadequate. Post-treatment RNA was extracted from FFPE scrolls of sections of the interface between treated and untreated tumor. RNA was normalized to 20ng/uL and hybridized with a target-specific Reporter and Capture Probes (CodeSet) with the nCounter Prep station at 65 °C for 18 hours. Sample data was acquired with the nCounter scanner. Background signal was reduced by subtracting threshold counts of 20 and normalization was performed with housekeeping genes using the nSolver 4.0 software.

3.2.3.3: Serum cytokine analysis

Multiplex serum cytokine analysis was performed using a commercially available canine-specific antibody-coated Bead-Based Multiplex Assay to quantify 13 cytokines in each sample (CCYTMG-90K-PX13, Millipore Sigma, Burlington, MA). The following cytokines were measured: GM-CSF, IFNg- IL-2, IL-6, IL-7, IL-8, IL-15, IP-10 (CXCL10), KC-like (CXCL1), IL-10, IL-18, MCP-1 (CCL2), and TNF-a. The assay was performed according to the manufacturer's directions. Samples were randomized on the plate. The samples were incubated overnight at 4°C and a magnetic plate washer was utilized. All standards, quality controls, and samples were analyzed in duplicate on Luminex® 200 multiplexing instruments (Luminex Corp, Austin, TX). Sample analyte concentrations were generated utilizing standard

curve data from each run via Belysa® curve fitting software (Millipore Sigma, Burlington, MA).

3.2.3.4: Statistical Analysis

Cytokine analysis results were evaluated for normal distribution with the D'Agostino's K-squared test. For normally distributed data, continuous variables were tested using the repeated-measures t-test, and categorical variables were tested using the Chi Square test. For skewed data, continuous variables were tested using either Wilcoxon test or the Cochran's Q test. Data for serum concentrations of inflammatory cytokines were normalized using $\log_{10}$ transformation and then analyzed using a paired, two-tailed t-test. All p-values were 2-sided, and p-values <0.05 were considered to be statistically significant. All cytokine statistical analyses were performed using GraphPad Prism 9 (GraphPad Software, San Diego, CA). The analytes pre- and/or post-treatment did not read for all patients and were excluded from statistical testing where appropriate.

For Nanostring gene expression results, sample values were log2 transformed to a variance plot to assess for differentially expressed (DE) genes using heteroscedastic *t* test ($p < 0.05$) per manufacturers' recommendations. DEs were analyzed using agglomerative clustering (Euclidean distance), fold changes and p values were reported for each DE on the ROSALIND™ software 3.35.40.

3.3 Results

3.3.1: Patient Population

Ten canine patients with spontaneous STS were enrolled in this study. Five female and five male dogs from different breeds (1 Boxer, 1 Bichon Frise, 1 Border Collie, 1 Great Dane,

1 Miniature Schnauzer, 1 Beagle, and 4 Mixed Breed Dogs) and aged 7-12 years received histotripsy treatment before surgical excision of the tumor 4 to 6 days after treatment. The characteristics of the canine patients, as well as, the grade, subtype, excision status, and location of the treated tumors are summarized in **Table I**.

In all dogs, the tumor was well visualized on the pretreatment CT scan and measured at least 2 cm in diameter. The histologic diagnosis of the tumors included 3 grade III STS, 4 grade II STS, 2 grade I STS, and 1 malignant mesenchymoma. For the tumors in which subtypes were included on the histopathology report, 3 perivascular wall tumors, 2 myxosarcoma, 1 malignant mesenchymoma, and 1 fibrosarcoma were diagnosed. After histotripsy treatment, eight dogs had their tumors completely excised with <0.1 – 0.5 cm margins where noted (margins not reported for all patients). In two dogs (Patients #1 and #2 is Table I), complete excision of the tumor was not achievable due to the extensive invasion of the tumor into healthy surrounding tissues and anatomic restrictions limiting the surgical window.

Patient outcome was followed for a median of 112 days (range: 14-285 days). Six dogs are still alive, three dogs were euthanized, and one dog was lost to follow up. All instances of euthanasia were determined to be unrelated to the histotripsy treatment. Two dogs were euthanized due to progressive disease typical of this disease: one had recurrence of the grade II STS and another had evidence of lung metastasis suspected secondary to the completely excised grade III STS. The third dog was euthanized due to development of a retrobulbar mass and immune mediated thrombocytopenia unrelated to the STS diagnosis.

3.3.2: Safety and Feasibility of Histotripsy Treatment

3.3.2.1: Adverse event assessment

No significant AEs impacting patient outcome were noted in any of the patients. Anesthesia complications unrelated to histotripsy were reported in three patients, resolving naturally or with standard intervention during treatment. Another patient experienced a vagal response from pain that may be secondary to histotripsy treatment, although the exact cause remains unknown. The remaining six patients had no anesthetic abnormalities. During treatment, body temperatures were maintained between 97.1˚F – 102.5˚F for nine patients with one patient experiencing moderate hypothermia at 96.4˚F that resolved with external heat. Pulse rates were maintained between 45-130 bpm for nine patients, with one patient experiencing cardiac dysrhythmia and an asystole cardiac rhythm. The suspected cause of this dysrhythmia is a vagal response from pain, as mentioned above, and the arrhythmia resolved on its own without any medical intervention. Mean blood pressures were maintained between 60-165 mmHg, with one patient experiencing persistent hypotension at 40 mmHg that resolved with fluid therapy. Oxygen saturation levels were maintained between 91-100%. End tidal carbon dioxide levels were maintained at 26-52 mmHg, with one patient experiencing persistent respiratory depression at 59 mmHg secondary to spontaneous breathing and resolved after increasing isoflurane gas. No complications (lethargy, fever, hypothermia) were reported during anesthetic recovery in any of the patients.

No clinically significant AEs associated with histotripsy treatment were reported through bloodwork, post-treatment physical examination, or owners' reports. On post-treatment physical examination, swelling was noted for five patients. The mass from nine patients were reported to be warm to the touch post-histotripsy treatment, and erythema of the

skin overlying the mass was recorded for five patients. The only histotripsy-related complications noted were various degrees of self-limiting cutaneous injury. Prior to treatment, nine patients had VCOG dermatology AE scores of 1, and one patient had a score of 4. Following histotripsy treatment, one patient (Patient #1) had an increase in VCOG dermatology AE score from 1 to 2, suspected to be due to pre-focal cavitation damage potential caused in part by hair left behind after shaving at the treatment site in this first patient [**Fig. 3**]. VCOG dermatology AE scores did not change after histotripsy for the remaining nine patients.

3.3.2.2: Histotripsy treatment outcomes

Automated histotripsy ablation treatments were applied to a spherical region within each of the targeted tumors at peak negative pressures (*p*-) averaging 22.60 ± 7.21 MPa. Depending on the size of the tumor, an ablation volume of either 4.14 cm^3, 8.18 cm^3, or 14.14 cm^3 was treated, corresponding to spherical diameters of 2 cm, 2.5 cm, and 3 cm, respectively. When possible, the histotripsy treatment volume was centered in the most solid region of the tumor (determined by pretreatment CT image analysis and physical examinations on the day of treatment). Planned treatment volumes are presented in **Table II**. Generation of clearly visible histotripsy cavitation bubble clouds on real-time ultrasound imaging was achieved in nine of ten treatments [**Fig. 3**]. The treatment without bubble cloud visibility was conducted through an intact surgical drape used to couple the patient's amorphous, ulcerated tumor to the degassed water bolus and the histotripsy transducer rather than the open acoustic window in the other nine patients. To confirm the presence of histotripsy cavitation at the targeted location in this dog, passive cavitation detection was used to measure the backscatter signal of the therapy pulse, similar to approaches used in previous histotripsy studies [44,88]. In all

subjects, cavitation activity was maintained for the duration of the volumetric histotripsy ablation. Treatment times correlated to the volume of the tumor treated, ranging from approximately 14 minutes to 1 hour in length for treatments of 4.19 cm^3 and 14.14 cm^3 in volume, respectively. No significant changes in the echogenicity of the treated regions were noted on ultrasound imaging post-treatment in any of the patients.

3.3.2.3: Computed tomography outcomes

Pre-treatment CT images identified clearly demarcated soft tissue tumors of at least 2 cm in diameter for all patients. All tumors had a least two regions of homogenous contrast uptake measuring at least 1 cm in diameter with an accessible treatment window. Comparison of pre- and post-treatment tumor sizes revealed a non-significant increase in tumor size that persisted 4-6 days after histotripsy treatment ($p = 0.191$ 1 day post- vs. pre-; $p = 0.077$ 4-6 day post- vs. pre-) [**Table II**]. Post-treatment CT images revealed clear, roughly spherical regions of histotripsy ablated tissue in seven of ten patients, visible on CT images as regions of decreased contrast uptake [**Fig. 3**]. In the three patients without visible ablation zones on CT, each animal had histologically-evident extensive tumor necrosis in the region of the treated tissue. Measurements of the ablation zone achieved by histotripsy treatment scaled according to planned ablation zone sizes (i.e., larger planned ablation volumes correlated with larger achieved ablation volumes), but measured ablation zones were often greater in size compared to the intended volume. Radiographically measured ablation volumes averaged 10.20 ± 18.18 cm^3 and 1.60 ± 10.75 cm^3 larger than planned volumes at 1 day and 4-6 days after treatment, respectively. Although measured volumes were larger than planned volumes when averaged across patients, measured ablation zone volumes were smaller than planned in some patients. Ablation zone volumes were non-significantly reduced 4 days after histotripsy relative to 1 day

post histotripsy ($p = 0.063$). Patients 2, 3, and 6 were excluded from analysis because no ablation zone could be definitively measured on CT images; patient 4 because no CT scan was collected 1-day post-histotripsy; and patient 8 because the post-treatment CT scan was taken on day 6. All other patients had 4-day post-histotripsy CT scans with discernable ablation zones.

3.3.2.4: Gross and histologic findings

After histotripsy, regions of ablation were clearly identified grossly and histologically in all samples. Grossly, treatment sites were characterized by extensive necrosis and regions of hemorrhage [**Fig. 4a**]. Histologic samples taken from treated regions of the tumors exhibited a mixture of lytic and coagulative cell death and an overall loss of viable tumor cells and cell nuclei, as well as, hemorrhage [**Fig. 4c**]. Clear boundaries were visible between untreated and treated areas of tissue [**Fig. 4d-f**].

Complete ablation was observed histologically in all ten dogs within the treated regions of the tumor. Occasionally, small foci of viable tumor cells centered near vessels and infiltrating immune cells, including neutrophils, were observed. No signs of histotripsy-induced damage were observed grossly or microscopically in untreated tissues, and no signs of thermal injury were observed within the treatment volumes or overlying tissues in any of the patients.

3.3.3: Tumor Microenvironment Following Ablation

3.3.3.1: Multiplex immunohistochemistry (mIHC) results

In more than half of all examined samples (7/10), mIHC investigating macrophage populations showed mild to marked increases in IBA-1 and CD206 double-positive cells (red) with macrophage morphology in sections taken from treated tumor [**Fig. 5**]. Moreover, in

untreated tumor samples, these cells were generally loosely distributed throughout intact tumor cells when present, while in treated samples, these often intensified at the interface between necrotic and intact tumor cells. In general, IBA-1/CD206 double positive macrophages were low within necrotic areas. All samples, both treated and untreated, were largely devoid of iNOS positive cells.

Lymphocyte analysis identified aggregates of CD3 positive cells in one tumor, the mesenchymoma, which were readily identifiable in treated samples but not present in untreated samples. Otherwise, there were generally no significant differences in the lymphocyte staining between treated and untreated sections.

3.3.3.2: Gene expression analysis

NanoString differential gene expression analysis identified 79 genes with at least a 2-fold upregulation between treated and untreated histotripsy groups. One patient (Patient #2) was excluded from statistical analysis because of low housekeeping gene expression. A gene set analysis was performed to group similar pathways. Myeloid compartment, NK cell functions, and interleukin gene sets obtained the highest significance score. Genes associated with inflammation, immune cell migration, and immune cell interactions were the highest upregulated [**Table III**]. Amongst the gene set analyses, the myeloid compartment gene sets obtained the highest significance score. Further analysis within the myeloid compartment gene sets showed the MARCO gene had the highest fold change. The protein encoded by this gene is a member of the class A scavenger receptor family and is part of the innate antimicrobial immune system. Overall, the gene set analysis indicated an immune-permissive tumor microenvironment.

3.3.4: Systemic Immune Response after Histotripsy

3.3.4.1: Serum cytokine analysis

Serum cytokine concentrations were compared pre-treatment and just prior to surgical resection of the tumor, four to six days post-treatment. There were no statistically-significant changes in the average patient serum cytokine concentrations following histotripsy treatment for any of the analytes. Individual patient serum cytokine concentrations were widely distributed for all analytes both pre- and post-treatment. Average serum cytokine concentrations ranged from 0.801 pg/mL (IFNg) to 3.605 pg/mL (IL-8) before histotripsy treatment and 1.088 pg/mL (IL-10) to 3.579 (IL-8) after histotripsy treatment for analytes IL-2, IL-6, IL-7, IL-8, IL-10, IL-15, IL-18, GMCSF, IFNg, TNFa, and MCP1. The average serum concentrations for analytes IP-10 and KC-like were higher in value, with values of 23.57 pg/mL and 541.3 pg/L pre-histotripsy and 21.04 pg/mL and 645.7 pg/mL after histotripsy treatment, respectively.

3.4 Discussion

This is the first study to demonstrate the safety and feasibility of histotripsy for superficial soft tissue sarcomas (STS). In all patients, histotripsy was successfully generated in the targeted regions, treatments were well-tolerated, and ablation of treated regions was observed. No significant adverse events associated with histotripsy were reported for any of the patients. Although histotripsy has been previously studied for the ablation of multiple tumor types [59-61,64,66,67,70], ablation of superficial tumors, including STS, presents a unique case for histotripsy due to the close proximity of the skin, which has the potential to be damaged by ablative therapies [74,75,89,90]. In this study, skin injury due to histotripsy was noted in the first

patient that was treated, with all subsequent treatments showing no change in the VCOG-CTCAE score after treatment. The observed skin injury in patient 1 corresponded to extensive pre-focal cavitation visible on real-time ultrasound imaging during treatment. During subsequent treatments, significant pre-focal cavitation was not seen on ultrasound imaging, suggesting that real-time imaging feedback can be used to monitor for these pre-focal cavitation events. Future work should consider optimized methods for preventing and monitoring pre-focal cavitation on the skin surface.

In all patients, histotripsy bubble clouds were successfully generated within the targeted tumor regions, resulting in precise ablation. The bubble clouds remained visible at the target location throughout the duration of the volumetric treatment and were visualized with real-time ultrasound imaging. After treatment, no significant changes to the echogenicity of the treated tissues were visible on as has been previously observed for histotripsy [91,92]. A comparison of pre- and post-treatment CT scans revealed clearly demarcated regions of histotripsy ablation in 7 of the 10 treated patients. In the final three patients, the ablated region could not be clearly visualized despite histologic confirmation of ablation. This finding suggests that MRI may be required to more accurately assess post-treatment histotripsy ablation in future studies, similar to prior histotripsy studies for other applications [93,94]. MRI is not a routine imaging modality for staging canine patients, but it is the standard imaging modality human STS patients [95]. In 7 of 10 patients, tumor size measured on CT images increased after histotripsy treatment, possibly due to transient swelling induced by histotripsy ablation. Similarly, post-treatment physical examination identified observable tumor swelling for five patients and tangible warmth of treated masses in nine patients. These findings may be a result of a pro-inflammatory immunogenic response locally in the treated tumor.

Radiographically measured ablation volumes were, on average, larger than planned volumes at 1 day and 4-6 days after treatment with no clear correlation between increased tumor sizes post-treatment and larger than planned ablation volumes. One potential explanation for this finding is that the treatment-induced ablation zone was able to stimulate further cell death in the tissue adjacent to the treatment zone in the 24 hours following histotripsy and before image acquisition. This scenario might also help to explain the aberrant edges to the ablation zone in some CT images. Four days after histotripsy, ablation zones decreased in size relative to one day after histotripsy. Although not statistically significant, this trend is consistent with prior histotripsy studies and suggests the ablation zone had begun to involute and be resorbed by the body. Previous studies characterizing the chronic response to histotripsy ablation in kidney and liver tissues have demonstrated that full resorption of the treated homogenate can take up to 1-2 months [54,85], making it likely that the ablated STS tissue would have been further resorbed if the tumors had not been surgically removed.

After surgical resection, ablation zones were grossly visible as regions of hemorrhage and necrosis in resected tissues, and histological analysis revealed a near complete removal of viable neoplastic cells in the treated region, with replacement by hemorrhage and acellular debris. In some patients, rare foci of viable tumor cells remained near blood vessels or near the boundaries of the treated lesions, suggesting that the histotripsy dose used in this study should be increased in future studies to ensure complete ablation of the entire targeted tumor volume. The acute immunological effects of histotripsy showed mild to marked increases in alternatively activated macrophages (M2) subjectively observed at the treatment interface. This increase may be due to the normal wound healing response, or possibly represent pro-tumoral tumor-associated macrophages. In the remodeling phase of normal wound healing, M2

macrophages predominate, expressing TGF-β and IL-10 to initiate resolution of inflammation and tissue repair [96]. However, tumor-associated macrophages (TAMs) of the M2 phenotype induced by IL-4 and IL-13 also promote angiogenesis, immune suppression, fibroblast proliferation, and stromal tissue remodeling, which are commonly observed in tumor progression, and may promote all steps of the metastatic cascade [97-99]. The inflammatory phase of wound healing peaks 24-48 hours after injury, with a significant reduction in neutrophils after three days and an increase in macrophages that facilitate tissue repair. Macrophage numbers remain high 2-7 days after injury, returning to steady state by day 14 [100]. In our study, post-treatment tumor samples were evaluated 4-6 days following histotripsy. Future studies should be conducted to quantify increases in M2-polarized macrophages and better elucidate their role following histotripsy at various time points after treatment.

Our results from the differential gene expression, routine H&E evaluation, and mIHC consistently reflect a state of inflammation, hemorrhage, and tissue remodeling following histotripsy treatment. The highest differentially expressed genes, MARCO, SERPINB2, CXCL8, and S100A8/9/12, indicate neutrophil chemotaxis, stress signaling, fibrin and coagulation, and anti-inflammatory (M2) macrophages. These findings are mirrored with the common finding of hemorrhage, hyalinization, and a subjective increase in M2-polarized macrophages. In one tumor sample, aggregates of CD3 positive cells were identified post-treatment. Accumulation of CD3 T lymphocytes is often present in wounds and can associated with the anti-inflammatory response and granulation tissue formation [101]. However, in the majority of samples, the mIHC lymphocyte panel revealed significant nonspecific staining of CD4 antibody within tumor cells, resulting in high background noise and obscuring other chromogen identification; thus, no conclusions can be drawn regarding lymphocyte tumor

infiltration post-treatment. Future studies may utilize other methods of immune cell quantification, such as flow cytometry or routine single-stain IHC techniques. Although there were no statistically significant differences between pre- and post-treatment cytokine concentrations for any of the analytes, it is possible that changes were missed due to the timing of cytokine data analysis in this study, which was conducted at various time points prior to histotripsy treatment and surgical removal. Prior studies have observed transient proinflammatory cytokine gene expression after FUS at time points ranging from 6-24 hours post-focused ultrasound [102,103]. For future studies, having standardized evaluation times obtained more frequently following histotripsy could better illustrate acute systemic immune changes, but can be difficult to achieve using a veterinary patient population due to scheduling constraints with owners.

These results are in line with previous investigations of histotripsy's immunostimulatory potential [46,57-62,71] and suggest that a single histotripsy ablation can alter the local tumor immune microenvironment. Notably, a recent study highlighted that there may be differences in the immune response depending on the percentage of the tumor treated with histotripsy [104]. In this study, histotripsy ablations were applied to either <25% or 50-75% of the total tumor volume in an orthotopic murine model of hepatocellular carcinoma. Decreased immune cell infiltration and delayed homogenate resorption were observed in the <25% group, suggesting that there may be a minimum tumor ablation volume required to generate meaningful immune effects [104]. In the current study, <25% of the total tumor volume was targeted in all ten canine patients. As a result, stronger immune trends may be identified following histotripsy ablation of increased volumes within patient tumors and should be investigated in future studies.

Overall, the results of this study suggest that histotripsy has the potential to be used as a non-invasive therapy for ablation and immunostimulation in patients with STS. However, future work remains to more extensively investigate histotripsy as a potential frontline therapy for STS. While this first treat-and-resect study provides invaluable insight into histotripsy's feasibility, patients still underwent surgery to remove their tumors. Additional studies are warranted to investigate whether histotripsy can ablate complete STS tumors with adequate margins to prevent local recurrence and achieve long-term outcomes equivalent to or superior to surgical resection. Similarly, since STS tumors can grow very large (>5 cm in diameter), and large STS size is a poor predictive factor making surgical resection more difficult [82], future histotripsy studies should explore methods for rapid volumetric ablation of STS tumors, such as previously investigated electronic focal steering methods [105-107]. Using this approach rather than mechanical steering of the focus through the treatment volume has previously been shown to significantly reduce treatment times by multiple orders of magnitude. For instance, a previous study by Lundt et al. showed a 40.7 ± 3.1 cm^3 volume could be ablated in 42 minutes at a treatment dose of 500 pulses [105]. Another potential approach to ablate large STS tumors is treating the tumor over separate, repeated sessions, similar to approaches used for fractionated radiation therapy treatments [108]. In addition to reducing the time per treatment session and lowering risks associated with prolonged anesthesia, applying repeated treatments might offer an added advantage of re-stimulating an already primed immune response to elicit additional systemic benefits. Repeated, partial treatments of the primary tumor might also avoid complications caused by ablation-related cytokine storms and/or immune cell hyperactivation, which could result from large volume ablations and have been observed for other ablation methods [109,110]. These potential methods for treating STS with histotripsy in single and

multiple sessions should be investigated in future trials, along with more extensive characterization of the chronic immune responses after partial and complete STS tumor ablation.

3.5: Conclusion

The results of this study demonstrate histotripsy's potential as a precise, non-invasive treatment for soft tissue sarcoma. This treat-and-resect study showed histotripsy was well-tolerated and effective in canine patients with spontaneous STS. Early immunological results suggest that histotripsy was able to induce pro-immunogenic changes in the local tumor microenvironment. Future trials investigating histotripsy for complete tumor ablation and characterizing the chronic response after histotripsy treatment are warranted.

List of Figures and Tables

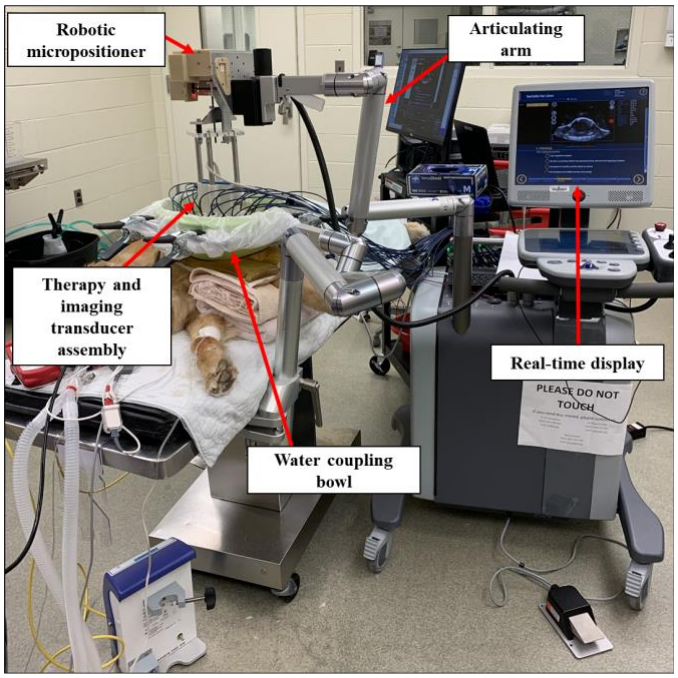

Fig. 1. Experimental histotripsy set-up. A robotic micro-positioner is connected to an articulating arm supporting the therapy and imaging transducer assembly. The transducer assembly was submerged in a water coupling bowl coupled to the patient's tumor, and treatment was monitored in real-time using ultrasound imaging.

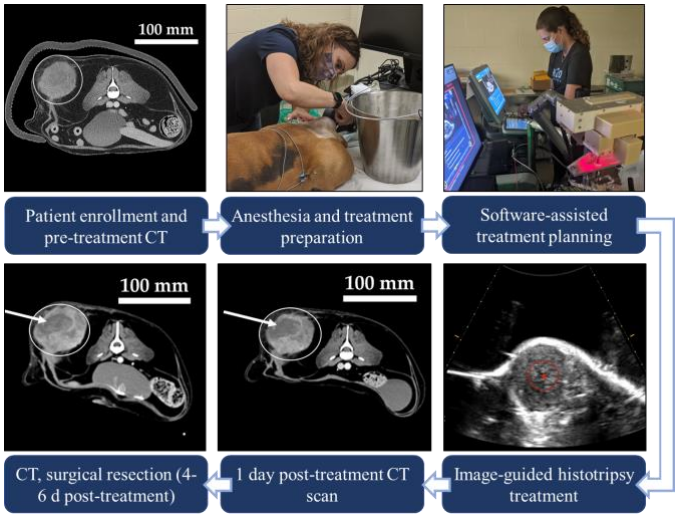

Fig. 2. Study workflow. After patient-specific treatment plan development, fur was removed and patients were anesthetized. An automated histotripsy treatment was conducted using custom planning software. Post-treatment images were collected before surgical resection of the tumor.

TABLE I. PATIENT DEMOGRAPHICS AND TUMOR CHARACTERISTICS

Patient #	Breed	Age (years)	Gender	Tumor Details	Tumor Location
1	Boxer	10	F	*PD:* Grade II STS *ST:* Perivascular wall tumor	Right caudodorsal proximal hind limb
2	Mixed Breed	10	M	*PD:* Grade II STS *ST:* Myxosarcoma	Right proximal hind limb
3	Bichon Frise	10	F	*PD:* Grade III STS	Right caudodorsal proximal hind limb
4	Mixed Breed	7	M	*PD:* Grade III STS	Left lateral elbow
5	Mixed Breed	12	F	*PD:* Grade I STS	Left craniolateral elbow
6	Miniature Schnauzer	10	M	*PD:* Grade III STS *ST:* Myxosarcoma	Left dorsal shoulder
7	Great Dane	10	F	*PD:* Grade II STS *ST:* Perivascular wall tumor	Left plantar metatarsus
8	Border Collie	11	M	*PD:* Malignant mesenchymoma *ST:* 3 lines of differentiation – osteoblast, fibroblast, lipoblast	Left medial hock
9	Mixed Breed	10	M	*PD:* Grade I STS *ST:* Perivascular wall tumor	Right lateral stifle
10	Beagle	12	F	*PD:* Grade II STS *ST:* Fibrosarcoma	Left lateral proximal hind limb

PD, primary diagnosis; ST, subtype.

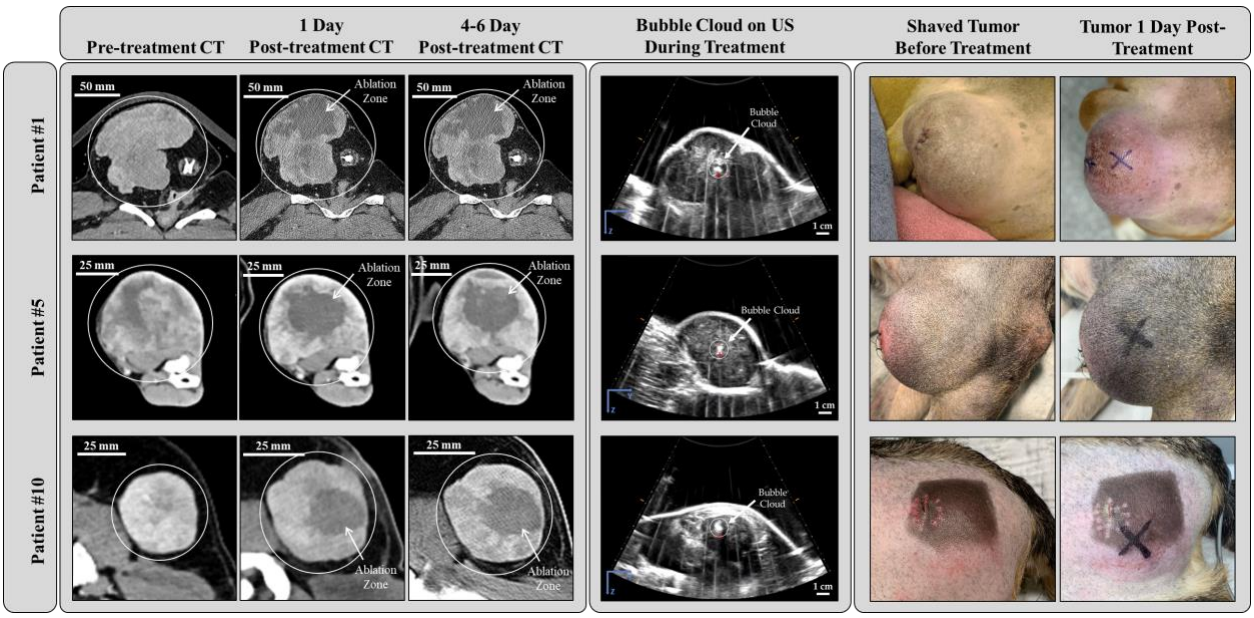

Fig. 3. Histotripsy treatment feasibility and safety were measured using CT and US imaging and adverse event monitoring. Representative images from three canine patients show (from left to right) pre-treatment CT scans of STS (circled), post-treatment CT images with clear regions of histotripsy-ablated tissue 1 day and 4 to 6 days after treatment (arrows), bubble clouds during treatment on real-time US imaging, and various degrees of self-limiting cutaneous injury in the histotripsy treatment path after treatment. Darkened skin on Patient #10 is the result of unrelated sun exposure prior to histotripsy treatment.

TABLE II. TUMOR AND ABLATION ZONE MEASUREMENTS PRE- AND POST-HISTOTRIPSY

Patient #	Tumor Dimensions (cm)			Ablation Zone Dimensions (cm)		
	Pre-treatment	1 Day Post-	4-6 Days Post-	Planned	1 Day Post-	4-6 Days Post-
1	8.5 x 8.5 x 8.8	9.9 x 8.4 x 10.2	9.2 x 9.3 x 9.9	3 x 3 x 3	5.0 x 4.8 x 4.8	4.7 x 3.9 x 4.0
2	14.6 x 10.1 x 14.1	16.1 x 10.7 x 15.3	16.7 x 11.4 x 16.2	2.5 x 2.5 x 2.5	Not visible*	Not visible*
3	5.5 x 4.6 x 4.6	5.3 x 4.5 x 4.6	5.5 x 4.2 x 4.3	2 x 2 x 2	Not visible*	Not visible*
4	9.2 x 6.5 x 8.4	N/A*	10.3 x 7.0 x 10.1	2.5 x 2.5 x 2.5	N/A**	1.3 x 2.0 x 2.0
5	6.7 x 4.3 x 6.9	6.7 x 4.2 x 7.0	6.9 x 4.5 x 7.0	2.5 x 2.5 x 2.5	3.2 x 2.7 x 2.7	3.3 x 3.0 x 2.8
6	16.5 x 6.4 x 9.8	N/A*	17.4 x 7.9 x 10.6	2.5 x 2.5 x 2.5	N/A**	Not visible*
7	8.4 x 5.4 x 5.5	8.5 x 5.8 x 6.2	8.6 x 6.6 x 6.8	2.5 x 2.5 x 2.5	3.4 x 3.2 x 3.1	1.7 x 2.1 x 1.8
8	8.1 x 3.9 x 2.3	8.1 x 3.6 x 2.6	8.0 x 3.3 x 2.6	2 x 2 x 2	2.0 x 1.5 x 1.8	1.2 x 0.8 x 1.1
9	3.7 x 3.4 x 3.1	3.8 x 3.4 x 3.0	3.4 x 3.3 x 3.1	2 x 2 x 2	1.8 x 1.3 x 1.3	1.0 x 0.9 x 0.9
10	5.3 x 4.1 x 3.8	5.0 x 3.9 x 3.9	5.4 x 4.1 x 4.1	2.5 x 2.5 x 2.5	3.1 x 3.0 x 2.8	2.8 x 2.0 x 2.2

Comparison of pre-, 1 day post-, and 4-6 day post-treatment tumor measurements and ablation zone dimensions as determined by CT imaging. *Ablation zones were not visible on CT scans. **Patients did not receive CT due to scheduling constraints.

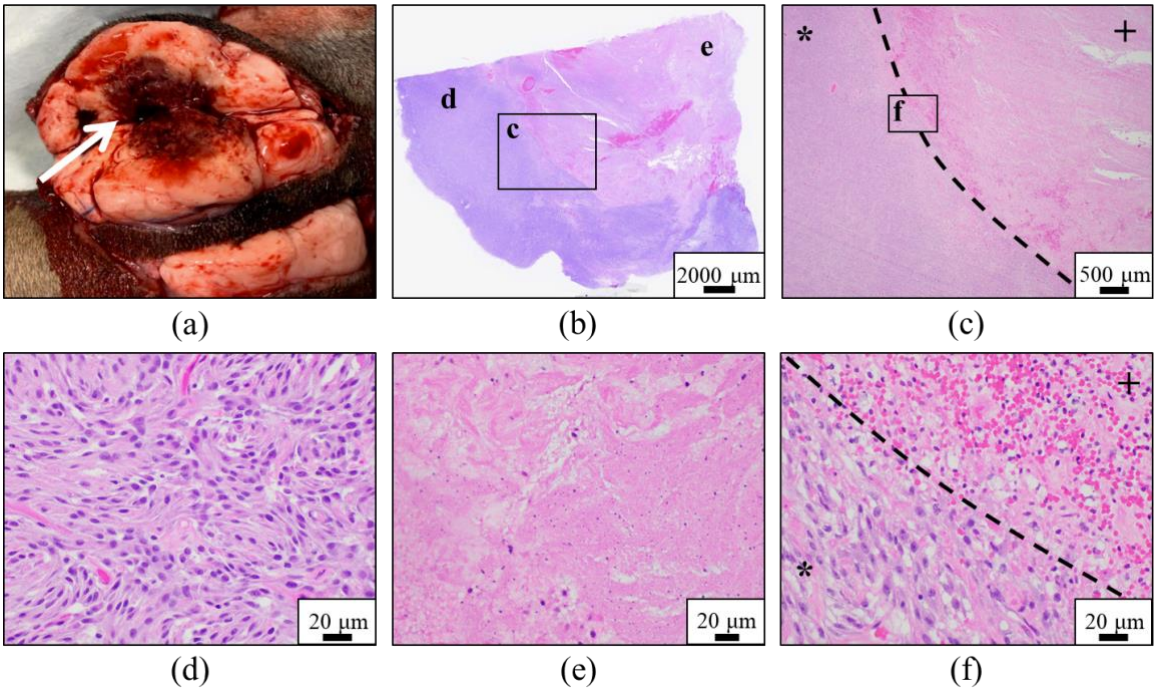

Fig. 4. Representative images demonstrating histotripsy ablation of STS for Patient #5. (a) Gross visualization of lesion characterized by extensive tissue necrosis and hemorrhage (arrow). (b-f) H&E stained sections compared (d) untreated (magnification 40x) and (e) treated (magnification

40x) tumor tissues and (b,c,f) interface regions (c – magnification 2x; f – magnification 40x). Clearly delineated boundaries between treated (+) and untreated (*) tumor tissue were observed

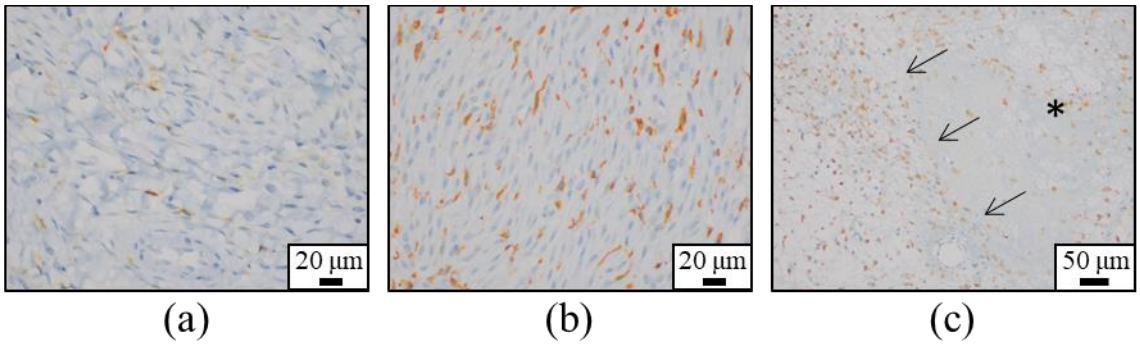

Fig. 5. Multiplex IHC to investigate macrophage populations following histotripsy. Lower numbers of IBA-1/CD206 double positive cells (orange/red) were distributed throughout untreated tumor samples (a) compared to treated samples (b). When captured, the interface between necrotic and intact tumor cells (c) often showed slightly increased numbers of double positive cells (* = area of necrosis; arrows = interface between necrotic and viable cells; a,b – magnification 40x; c – magnification 20x).

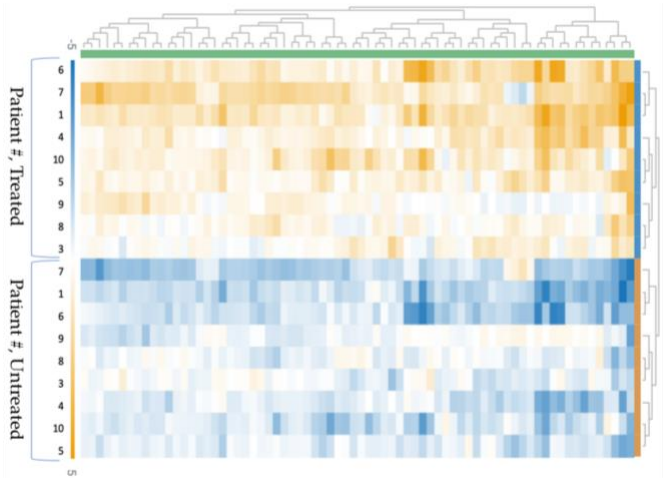

Fig. 6. Hierarchical clustering of 79 differentially expressed immuno-oncology genes. Increasing orange intensity indicates increased gene expression and increasing blue intensity indicates decreased gene expression, as shown in the scale bar. According to the differential gene expression profile, samples were clustered with patient held as a confounder and arranged with the treated samples at the top of the figure (blue bar) and the untreated samples at the bottom of the figure (yellow bar).

TABLE III. DESCRIPTION AND FOLD CHANGES FOR TOP 20 DIFFERENTIALLY EXPRESSED GENES

Gene	Description	Fold Change	Adjusted P-value
MARCO	Macrophage receptor with collagenous structure	37.2986	0.00238
SERPINB2	Serpin peptidase inhibitor, clade B (ovalbumin), member 2	24.1843	0.00350
CXCL8	Interleukin 8	17.1997	0.00350
MMP1	Interstitial collagenase-like	13.2284	0.00583
LOC106557449	Alveolar macrophage chemotactic factor-like	12.5658	0.00382
S100A12	S100 calcium binding protein A12	12.3522	0.00636
PTGS2	Prostaglandin-endoperoxide synthase 2 (prostaglandin G/H synthase and cyclooxygenase)	6.73748	0.00656
IL6	Interleukin 6 (interferon, beta 2)	6.36584	0.01566
OSM	Oncostatin M	6.24945	0.00350
S100A9	S100 calcium binding protein A9	5.41560	0.01772
S100A8	S100 calcium binding protein A8	5.19232	0.01440
ITGAM	Integrin, alpha M (complement component 3 receptor 3 subunit)	4.85863	0.00982
CCL8	Chemokine (C-C motif) ligand 8	4.56590	0.00583
TREM1	Triggering receptor expressed on myeloid cells 1	4.12716	0.00442
CSF3R	Colony stimulating factor 3 receptor (granulocyte)	4.07322	0.00715
MMP9	Matrix metallopeptidase 9 (gelatinase B, 92 kDa gelatinase, 92 kDa type IV collagense)	4.05682	0.02271
CMA1	Chymase 1, mast cell	3.88695	0.02563
GATA3	GATA binding protein 3	3.87514	0.03998
IL23R	Interleukin 23 receptor	3.80119	0.00656
IL18R	Interleukin 18 receptor 1	3.7024	0.01054

References

1. Ehrhart N. Soft-tissue sarcomas in dogs: a review. (1547-3317 (Electronic))
2. Gamboa AC, Gronchi A, Cardona K. Soft-tissue sarcoma in adults: An update on the current state of histiotype-specific management in an era of personalized medicine. *CA Cancer J Clin*. May 2020;70(3):200-229. doi:10.3322/caac.21605
3. Séguin B. Canine Soft Tissue Sarcomas: Can Being a Dog's Best Friend Help a Child? (2234-943X (Print))
4. Dennis MM, McSporran KD, Bacon NJ, Schulman FY, Foster RA, Powers BE. Prognostic Factors for Cutaneous and Subcutaneous Soft Tissue Sarcomas in Dogs. *Veterinary Pathology*. 2023/01/02 2010;48(1):73-84. doi:10.1177/0300985810388820
5. Ettinger SN, Scase Tj Fau - Oberthaler KT, Oberthaler Kt Fau - Craft DM, et al. Association of argyrophilic nucleolar organizing regions, Ki-67, and proliferating cell nuclear antigen scores with histologic grade and survival in dogs with soft tissue sarcomas: 60 cases (1996-2002). (0003-1488 (Print))
6. Goldschmidt MH, Hendrick MJCp. Tumors of the Skin and Soft Tissues. 2002:45-117. doi:https://doi.org/10.1002/9780470376928.ch2
7. Foale RD, White Ra Fau - Harley R, Harley R Fau - Herrtage ME, Herrtage ME. Left ventricular myxosarcoma in a dog. (0022-4510 (Print))
8. Richter M, Stankeova S Fau - Hauser B, Hauser B Fau - Scharf G, Scharf G Fau - Spiess BM, Spiess BM. Myxosarcoma in the eye and brain in a dog. (1463-5216 (Print))
9. Iwaki YA-O, Lindley S, Smith A, Curran KM, Looper J. Canine myxosarcomas, a retrospective analysis of 32 dogs (2003-2018). (1746-6148 (Electronic))
10. Fulmer AK, Mauldin GE. Canine histiocytic neoplasia: an overview. (0008-5286 (Print))
11. Waters CB, Morrison Wb Fau - DeNicola DB, DeNicola Db Fau - Widmer WR, Widmer Wr Fau - White MR, White MR. Giant cell variant of malignant fibrous histiocytoma in dogs: 10 cases (1986-1993). (0003-1488 (Print))
12. Morris JS, McInnes Ef Fau - Bostock DE, Bostock De Fau - Hoather TM, Hoather Tm Fau - Dobson JM, Dobson JM. Immunohistochemical and histopathologic features of 14 malignant fibrous histiocytomas from Flat-Coated Retrievers. (0300-9858 (Print))
13. Avallone G, Helmbold P Fau - Caniatti M, Caniatti M Fau - Stefanello D, Stefanello D Fau - Nayak RC, Nayak Rc Fau - Roccabianca P, Roccabianca P. The spectrum of canine cutaneous perivascular wall tumors: morphologic, phenotypic and clinical characterization. (0300-9858 (Print))
14. Chijiwa K, Uchida K Fau - Tateyama S, Tateyama S. Immunohistochemical evaluation of canine peripheral nerve sheath tumors and other soft tissue sarcomas. (0300-9858 (Print))
15. Teixeira S, Amorim I, Rêma A, Faria F, Gärtner F. Molecular Heterogeneity of Canine Cutaneous Peripheral Nerve Sheath Tumors: A Drawback in the Diagnosis Refinement. (1791-7549 (Electronic))
16. Brehm DM, Vite Ch Fau - Steinberg HS, Steinberg Hs Fau - Haviland J, Haviland J Fau - van Winkle T, van Winkle T. A retrospective evaluation of 51 cases of peripheral nerve sheath tumors in the dog. (0587-2871 (Print))
17. Baez JL, Hendrick Mj Fau - Shofer FS, Shofer Fs Fau - Goldkamp C, Goldkamp C Fau - Sorenmo KU, Sorenmo KU. Liposarcomas in dogs: 56 cases (1989-2000). (0003-1488 (Print))

18. Caserto BG. A comparative review of canine and human rhabdomyosarcoma with emphasis on classification and pathogenesis. (1544-2217 (Electronic))
19. Cooper BJ VB. Tumors in domestic animals: Tumors of muscle. Iowa State Press; 2002. p. 319-363.
20. Kobayashi M, Sakai H Fau - Hirata A, Hirata A Fau - Yonemaru K, et al. Expression of myogenic regulating factors, Myogenin and MyoD, in two canine botryoid rhabdomyosarcomas. (0300-9858 (Print))
21. Curran KM, Halsey CH, Worley DR. Lymphangiosarcoma in 12 dogs: a case series (1998-2013). (1476-5829 (Electronic))
22. Halsey CH, Worley DR, Curran K, Charles JB, Ehrhart EJ. The use of novel lymphatic endothelial cell-specific immunohistochemical markers to differentiate cutaneous angiosarcomas in dogs. (1476-5829 (Electronic))
23. McDonald Rk Fau - Helman RG, Helman RG. Hepatic malignant mesenchymoma in a dog. (0003-1488 (Print))
24. Watson AD, Young Km Fau - Dubielzig RR, Dubielzig Rr Fau - Biller DS, Biller DS. Primary mesenchymal or mixed-cell-origin lung tumors in four dogs. (0003-1488 (Print))
25. Ghisleni G, Roccabianca P Fau - Ceruti R, Ceruti R Fau - Stefanello D, et al. Correlation between fine-needle aspiration cytology and histopathology in the evaluation of cutaneous and subcutaneous masses from dogs and cats. (0275-6382 (Print))
26. McSporran KD. Histologic grade predicts recurrence for marginally excised canine subcutaneous soft tissue sarcomas. (1544-2217 (Electronic))
27. Kuntz CA, Dernell Ws Fau - Powers BE, Powers Be Fau - Devitt C, Devitt C Fau - Straw RC, Straw Rc Fau - Withrow SJ, Withrow SJ. Prognostic factors for surgical treatment of soft-tissue sarcomas in dogs: 75 cases (1986-1996). (0003-1488 (Print))
28. Chase D, Bray J Fau - Ide A, Ide A Fau - Polton G, Polton G. Outcome following removal of canine spindle cell tumours in first opinion practice: 104 cases. (1748-5827 (Electronic))
29. Baker-Gabb M, Hunt Gb Fau - France MP, France MP. Soft tissue sarcomas and mast cell tumours in dogs; clinical behaviour and response to surgery. (0005-0423 (Print))
30. Del Magno SA-O, Morello E, Iussich S, et al. Evaluation of the neoplastic infiltration of the skin overlying canine subcutaneous soft tissue sarcomas: An explorative study. (1476-5829 (Electronic))
31. Forrest LJ, Chun R Fau - Adams WM, Adams Wm Fau - Cooley AJ, Cooley Aj Fau - Vail DM, Vail DM. Postoperative radiotherapy for canine soft tissue sarcoma. (0891-6640 (Print))
32. McKnight JA, Mauldin Gn Fau - McEntee MC, McEntee Mc Fau - Meleo KA, Meleo Ka Fau - Patnaik AK, Patnaik AK. Radiation treatment for incompletely resected soft-tissue sarcomas in dogs. (0003-1488 (Print))
33. Simon D, Ruslander Dm Fau - Rassnick KM, Rassnick Km Fau - Wood CA, et al. Orthovoltage radiation and weekly low dose of doxorubicin for the treatment of incompletely excised soft-tissue sarcomas in 39 dogs. (0042-4900 (Print))
34. Crownshaw Ah Fau - McEntee MC, McEntee Mc Fau - Nolan MW, Nolan Mw Fau - Gieger TL, Gieger TL. Evaluation of variables associated with outcomes in 41 dogs with incompletely excised high-grade soft tissue sarcomas treated with definitive-intent radiation therapy with or without chemotherapy. (1943-569X (Electronic))

35. Gagnon J Fau - Mayer MN, Mayer Mn Fau - Belosowsky T, Belosowsky T Fau - Mauldin GN, Mauldin Gn Fau - Waldner CL, Waldner CL. Stereotactic body radiation therapy for treatment of soft tissue sarcomas in 35 dogs. (1943-569X (Electronic))
36. Selting KA, Powers Be Fau - Thompson LJ, Thompson Lj Fau - Mittleman E, et al. Outcome of dogs with high-grade soft tissue sarcomas treated with and without adjuvant doxorubicin chemotherapy: 39 cases (1996-2004). (0003-1488 (Print))
37. Elmslie RE, Glawe P Fau - Dow SW, Dow SW. Metronomic therapy with cyclophosphamide and piroxicam effectively delays tumor recurrence in dogs with incompletely resected soft tissue sarcomas. (0891-6640 (Print))
38. Schiffman JD, Breen M. Comparative oncology: what dogs and other species can teach us about humans with cancer. *Philos Trans R Soc Lond B Biol Sci*. Jul 19 2015;370(1673)doi:10.1098/rstb.2014.0231
39. LeBlanc AK, Mazcko CN. Improving human cancer therapy through the evaluation of pet dogs. *Nat Rev Cancer*. Dec 2020;20(12):727-742. doi:10.1038/s41568-020-0297-3
40. van der Weyden L, Brenn T, Patton EE, Wood GA, Adams DJ. Spontaneously occurring melanoma in animals and their relevance to human melanoma. *The Journal of pathology*. Sep 2020;252(1):4-21. doi:10.1002/path.5505
41. Wu Y, Chang YM, Polton G, et al. Gene Expression Profiling of B Cell Lymphoma in Dogs Reveals Dichotomous Metabolic Signatures Distinguished by Oxidative Phosphorylation. *Front Oncol*. 2020;10:307. doi:10.3389/fonc.2020.00307
42. Zhou YF. High intensity focused ultrasound in clinical tumor ablation. *World J Clin Oncol*. Jan 10 2011;2(1):8-27. doi:10.5306/wjco.v2.i1.8
43. Hoogenboom M, Eikelenboom D, den Brok MH, Heerschap A, Futterer JJ, Adema GJ. Mechanical high-intensity focused ultrasound destruction of soft tissue: working mechanisms and physiologic effects. *Ultrasound Med Biol*. Jun 2015;41(6):1500-17. doi:10.1016/j.ultrasmedbio.2015.02.006
44. Vlaisavljevich E, Lin KW, Maxwell A, et al. Effects of ultrasound frequency and tissue stiffness on the histotripsy intrinsic threshold for cavitation. *Ultrasound Med Biol*. Jun 2015;41(6):1651-67. doi:10.1016/j.ultrasmedbio.2015.01.028
45. van den Bijgaart RJ, Eikelenboom DC, Hoogenboom M, Futterer JJ, den Brok MH, Adema GJ. Thermal and mechanical high-intensity focused ultrasound: perspectives on tumor ablation, immune effects and combination strategies. *Cancer immunology, immunotherapy : CII*. Feb 2017;66(2):247-258. doi:10.1007/s00262-016-1891-9
46. Ho YJ, Li JP, Fan CH, Liu HL, Yeh CK. Ultrasound in tumor immunotherapy: Current status and future developments. *J Control Release*. Jul 10 2020;323:12-23. doi:10.1016/j.jconrel.2020.04.023
47. Carroll J. C-OS, Barry S., Klahn S, Allen I, Ruth J, Dervisis N. First-in-patient trial of high intensity focused ultrasound (HIFU) for treatment of canine solid tumors. 2020:
48. Hoogenboom M, Eikelenboom D, den Brok M, Heerschap A, Futterer J, Adema G. Mechanical high-intensity focused ultrasound destruction of soft tissue: working mechanisms and physiologic effects. *Ultrasound in Medicine & Biology*. 2015;41(6):1500-17. doi:10.1016/j.ultrasmedbio.2015.02.006

49. Bader K, Vlaisavljevich E, Maxwell A. For Whom the Bubble Grows: Physical Principles of Bubble Nucleation and Dynamics in Hisotripsy Ultrasound Therapy. *Ultrasound Med Biol*. 2019;45(5)doi:10.1016/j.ultrasmedbio.2018.10.035
50. Vlaisavljevich E, Maxwell A, Mancia L, Johnsen E, Cain C, Xu Z. Visualizing the Histotripsy Process: Bubble Cloud-Cancer Cell Interactions in a Tissue-Mimicking Environment. *Ultrasound Med Biol*. 2016;42(10):2466-2477. doi:10.1016/j.ultrasmedbio.2016.05.018. Epub 2016 Jul 9. PMID: 27401956; PMCID: PMC5010997
51. Xu Z, Hall TL, Vlaisavljevich E, Lee Jr FT. Histotripsy: the first noninvasive, non-ionizing, non-thermal ablation technique based on ultrasound. *Int J Hyperthermia*. 2021;38(1):561-575. doi:https://doi.org/10.1080/02656736.2021.1905189
52. Vlaisavljevich E, Maxwell A, Warnez M, Johnsen E, Cain CA, Xu Z. Histotripsy-induced cavitation cloud initiation thresholds in tissues of different mechanical properties. *IEEE Trans Ultrason Ferroelectr Freq Control*. Feb 2014;61(2):341-52. doi:10.1109/TUFFC.2014.6722618
53. Vlaisavljevich E, Lin K-W, Warnez MT, et al. Effects of tissue stiffness, ultrasound frequency, and pressure on histotripsy-induced cavitation bubble behavior. *Phys Med Biol*. 2015;60(6):2271-2292. doi:10.1088/0031-9155/60/6/2271
54. Hall T, Kieran K, Ives K, Fowlkes J, Cain C, Roberts W. Histotripsy of rabbit renal tissue in vivo: temporal histologic trends. *J Endourol*. 2007;21(10):1159-1166. doi:10.1089/end.2007.9915
55. Iro H, Völklein Ba Fau - Waldfahrer F, Waldfahrer F Fau - Schneider T, Schneider T Fau - Riedlinger RE, Riedlinger Re Fau - Zenk J, Zenk J. Cytotoxic and anti-proliferative effects of high-energy pulsed ultrasound (HEPUS) on human squamous cell carcinoma cells as compared to connective tissue fibroblasts. (0937-4477 (Print))
56. Hall TL, Hempel Cr Fau - Wojno K, Wojno K Fau - Xu Z, Xu Z Fau - Cain CA, Cain Ca Fau - Roberts WW, Roberts WW. Histotripsy of the prostate: dose effects in a chronic canine model. (1527-9995 (Electronic))
57. Hendricks-Wenger A, Hutchison R, Vlaisavljevich E, Allen IC. Immunological Effects of Histotripsy for Cancer Therapy. Review. *Front Oncol*. 2021-May-31 2021;11(1999)doi:10.3389/fonc.2021.681629
58. Qu S, Worlikar T, Felsted AE, et al. Non-thermal histotripsy tumor ablation promotes abscopal immune responses that enhance cancer immunotherapy. *J Immunother Cancer*. 2020;8(1)
59. Hendricks-Wenger A, Sereno J, Gannon J, et al. Histotripsy Ablation Alters the Tumor Microenvironment and Promotes Immune System Activation in a Subcutaneous Model of Pancreatic Cancer. *IEEE Transactions on Ultrasonics, Ferroelectrics, and Frequency Control*. 2021;
60. Vidal JJ, Vlaisavljevich E, Cannata J, et al. Phase I Study of Safety and Efficacy of Hepatic Histotripsy: Preliminary Results of First in Man Experience with Robotically-Assisted Sonic Therapy. 2019:
61. Schade G, Wang Y, D'Andrea S, Hwang J, Liles W, Khokhlova T. Boiling Histotripsy Ablation of Renal Cell Carcinoma in the Eker Rat Promotes a Systemic Inflammatory Response. *Ultrasound Med Biol*. 2019;45(1):137-147. doi:10.1016/j.ultrasmedbio.2018.09.006

62. Pahk K, Shin C, Bae I, et al. Boiling Histotripsy-induced Partial Mechanical Ablation Modulates Tumour Microenvironment by Promoting Immunogenic Cell Death of Cancers. *Sci Rep*. 2019;9(9050)
63. Qu S, Worlikar T, Felsted AE, et al. Non-thermal histotripsy tumor ablation promotes abscopal immune responses that enhance cancer immunotherapy. *J Immunother Cancer*. Jan 2020;8(1)doi:10.1136/jitc-2019-000200
64. Schade G, Keller J, Ives K, et al. Histotripsy focal ablation of implanted prostate tumor in an ACE-1 canine cancer model. *J Urol*. 2012;188(5):1957-1964. doi:10.1016/j.juro.2012.07.006
65. Gerhardson T, Pal A, Sheetz L, et al. Histotripsy Mediated Immunomodulation in a Mouse GL261 Intracranial Glioma Model. 2018:
66. Worlikar T, Vlaisavljevich E, Gerhardson T, et al. Histotripsy for Non-Invasive Ablation of Hepatocellular Carcinoma (HCC) Tumor in a Subcutaneous Xenograft Murine Model. *Conference Proceedings - IEEE Engineering in Medicine and Biology Society*. 2018;2018:6064-6067. doi:10.1109/EMBC.2018.8513650
67. Hendricks-Wenger A, Weber P, Simon A, et al. Histotripsy for the Treatment of Cholangiocarcinoma Liver Tumors: In Vivo Feasibility and Ex Vivo Dosimetry Study. *IEEE Transactions on Ultrasonics, Ferroelectrics, and Frequency Control*. 2021;
68. Vidal-Jove J, Serres X, Vlaisavljevich E, et al. First-in-man histotripsy of hepatic tumors: the THERESA trial, a feasibility study. (1464-5157 (Electronic))
69. Ruger LY, Ester, Coutermarsh-Ott S, Vickers E, et al. Histotripsy Ablation for the Treatment of Feline Injection Site Sarcomas: A First-in-Cat In Vivo Feasibility Study. TechRxiv. Prepint.2023.
70. Arnold L, Hendricks-Wenger A, Coutermarsh-Ott S, et al. Histotripsy Ablation of Bone Tumors: Feasibility Study in Excised Canine Osteosarcoma Tumors. *Ultrasound in Medicine & Biology*. 2021;47(12):3435-3446. doi:https://doi.org/10.1016/j.ultrasmedbio.2021.08.004
71. Vidal JJ, Serres-Creixams X, Ziemlewicz TJ, Cannata JM. Liver Histotripsy Mediated Abscopal Effect—Case Report. *IEEE Transactions on Ultrasonics, Ferroelectrics, and Frequency Control*. 2021;68(9):3001-3005. doi:10.1109/TUFFC.2021.3100267
72. Antoniou A, Evripidou N, Panayiotou S, Spanoudes K, Damianou C. Treatment of canine and feline sarcoma using MR-guided focused ultrasound system. *Journal of Ultrasound*. 2022;doi:https://doi.org/10.1007/s40477-022-00672-5
73. Seward MC, Daniel GB, Ruth JD, Dervisis N, Partanen A, Yarmolenko PS. Feasibility of targeting canine soft tissue sarcoma with MR-guided high-intensity focused ultrasound. *Int J Hyperthermia*. 2019;35(1):205-215. doi:10.1080/02656736.2018.1489072
74. Wu F, Wang Z, Chen W, et al. Extracorporeal focused ultrasound surgery for treatment of human solid carcinomas: early Chinese clinical experience. *Ultrasound Med Biol*. 2004;30(2):245-260. doi:doi: 10.1016/j.ultrasmedbio.2003.10.010
75. Yu W, Tang L, Lin F, Jiang L, Shen Z. Significance of HIFU in local unresectable recurrence of soft tissue sarcoma, a single-center, respective, case series in China. *Surg Oncol*. 2019;30:117-121. doi:https://doi.org/10.1016/j.suronc.2019.06.004
76. Shim J, Staruch RM, Koral K, Xie X, Chopra R, Laetsch T. Pediatric Sarcomas Are Targetable by MR-Guided High Intensity Focused Ultrasound (MR-HIFU): Anatomical Distribution and Radiological Characteristics. *Pediatr Blood Cancer*. 2016;63(10):1753-1760. doi:https://doi.org/10.1002/pbc.26079

77. Hendricks-Wenger A, Arnold L, Gannon J, et al. Histotripsy Ablation in Preclinical Animal Models of Cancer and Spontaneous Tumors in Veterinary Patients: A Review. *IEEE TRANSACTIONS ON ULTRASONICS, FERROELECTRICS, AND FREQUENCY CONTROL*. 2022;69(1):5-26. doi:10.1109/TUFFC.2021.3110083
78. Carvalho MI, Raposo TP, Silva-Carvalho R, et al. The Dog as a Model to Study the Tumor Microenvironment. *Advances in experimental medicine and biology*. 2021;1329:123-152. doi:10.1007/978-3-030-73119-9_7
79. McCarthy CE ZN, Elijanne M, Sharon E, Voest EE, Palucka K. Developing and validating model systems for immuno-oncology. *Cancer cell*. 2021;39(8):1018-1022.
80. Von Rueden SK, Fan TM. Cancer-Immunity Cycle and Therapeutic Interventions-Opportunities for Including Pet Dogs With Cancer. *Front Oncol*. 2021;11:773420. doi:10.3389/fonc.2021.773420
81. Panjwani MK, Atherton MJ, MaloneyHuss MA, et al. Establishing a model system for evaluating CAR T cell therapy using dogs with spontaneous diffuse large B cell lymphoma. *Oncoimmunology*. 2020;9(1):1676615. doi:10.1080/2162402X.2019.1676615
82. Dennis MM, McSporran KD, Bacon NJ, Schulman FY, Foster RA, Powers BE. Prognostic factors for cutaneous and subcutaneous soft tissue sarcomas in dogs. *Veterinary Pathology*. 2011;48(1):73-84. doi:https://doi.org/10.1177/0300985810388820
83. Parsons J, Cain C, Fowlkes JB. Cost-effective assembly of a basic fiber-optic hydrophone for measurement of high-amplitude therapeutic ultrasound fields. *J Acoust Soc Am*. 2006;119(3):1432-1440.
84. Parsons JE, Cain CA, Abrams GD, Fowlkes JB. Pulsed cavitational ultrasound therapy for controlled tissue homogenization. *Ultrasound Med Biol*. Jan 2006;32(1):115-29. doi:10.1016/j.ultrasmedbio.2005.09.005
85. Vlaisavljevich E, Greve J, Cheng X, et al. Non-Invasive Ultrasound Liver Ablation Using Histotripsy: Chronic Study in an In Vivo Rodent Model. *Ultrasound Med Biol*. 2016;42(8):1890-1902. doi:10.1016/j.ultrasmedbio.2016.03.018
86. Vlaisavljevich E, Kim Y, Allen S, et al. Image-Guided Non-Invasive Ultrasound Liver Ablation Using Histotripsy: Feasibility Study in an *in vivo* Porcine Model. *Ultrasound Med Biol*. 2013;39(8):1398-1409. doi:https://dx.doi.org/10.1016%2Fj.ultrasmedbio.2013.02.005
87. LeBlanc AK, Atherton M, Bentley RT, et al. Veterinary Cooperative Oncology Group-Common Terminology Criteria for Adverse Events (VCOG-CTCAE v2) following investigational therapy in dogs and cats. *Vet Comp Oncol*. 2021;19(2):311-352. doi:https://doi.org/10.1111/vco.12677
88. Zhang X, Jin L, Vlaisavljevich E, et al. Non-invasive Thrombolysis using Microtripsy: A Parameter Study. *IEEE Trans Ultrason Ferroelectr Freq Control*. 2015;62(12):2092-2105. doi:10.1109/TUFFC.2015.007268
89. Li J-J, Gu M-F, Luo G-Y, Liu L-Z, Zhang R, Xu G-L. Complications of High Intensity Focused Ultrasound for Patients with Hepatocellular Carcinoma. *Technology in Cancer Research and Treatment*. 2009;8(3):217-224. doi:https://doi.org/10.1177%2F153303460900800306
90. Huffman SD, Huffman NP, Lewandowski RJ, Brown DB. Radiofrequency Ablation Complicated by Skin Burn. *Complications in Interventional Oncology*. 2011;28(2):179-182. doi:https://dx.doi.org/10.1055%2Fs-0031-1280660

91. Hall TL, Fowlkes JB, Cain CA. Imaging feedback of tissue liquefaction (histotripsy) in ultrasound surgery. 2005:1732-1734.
92. Hall TL, Fowlkes JB. A real-time measure of cavitation induced tissue disruption by ultrasound imaging backscatter reduction. *IEEE Transactions on Ultrasonics, Ferroelectrics, and Frequency Control*. 2007;54(3):569-575. doi:https://doi.org/10.1109/TUFFC.2007.279
93. Smolock AR, Cristescu MM, Vlaisavljevich E, et al. Robotically Assisted Sonic Therapy as a Noninvasive Nonthermal Ablation Modality: Proof of Concept in a Porcine Liver Model. *Radiology*. May 2018;287(2):485-493. doi:10.1148/radiol.2018171544
94. Allen S, Vlaisavljevich E, Shi J, et al. The response of MRI contrast parameters in in vitro tissues and tissue mimicking phantoms to fractionation by histotripsy. *Phys Med Biol*. 2017;62(17):7167-7180. doi:10.1088/1361-6560/aa81ed
95. Kotilingam D, Lev DC, Lazar AJF, Pollock RE. Staging soft tissue sarcoma: evolution and change. *CA: a cancer journal for clinicians*. 2006;56(5):282-291. doi:10.3322/canjclin.56.5.282
96. Hua Y, Bergers G. Tumors vs. Chronic Wounds: An Immune Cell's Perspective. *Front Immunol*. 2019;10:2178. doi:10.3389/fimmu.2019.02178
97. Liu J, Geng X, Hou J, Wu G. New insights into M1/M2 macrophages: key modulators in cancer progression. *Cancer Cell Int*. 2021;21(1):389. doi:10.1186/s12935-021-02089-2
98. Deng Y, Hu JC, He SH, et al. Sphingomyelin synthase 2 facilitates M2-like macrophage polarization and tumor progression in a mouse model of triple-negative breast cancer. *Acta Pharmacol Sin*. Jan 2021;42(1):149-159. doi:10.1038/s41401-020-0419-1
99. Lin Y, Xu J, Lan H. Tumor-associated macrophages in tumor metastasis: biological roles and clinical therapeutic applications. *J Hematol Oncol*. 2019;12(1):76. doi:10.1186/s13045-019-0760-3
100. Aitcheson S, Frentiu F, Hurn S, Edwards K, Murray R. Skin Wound Healing: Normal Macrophage Function and Macrophage Dysfunction in Diabetic Wounds. *Molecules*. 2021;26(16):4917. doi:10.3390/molecules26164917
101. Wang X, Balaji S, Steen E, et al. T Lymphocytes Attenuate Dermal Scarring by Regulating Inflammation, Neovascularization, and Extracellular Matrix Remodeling. *Adv Wound Care (New Rochelle)*. 2019;8(11):527-537. doi:10.1089/wound.2019.0981
102. McMahon D, Bendayan R, Hynynen K. Acute effects of focused ultrasound-induced increases in blood-brain barrier permeability on rat microvascular transcriptome. *Sci Rep*. Apr 4 2017;7:45657. doi:10.1038/srep45657
103. Kovacs ZI, Kim S, Jikaria N, et al. Disrupting the blood-brain barrier by focused ultrasound induces sterile inflammation. *Proc Natl Acad Sci U S A*. Jan 3 2017;114(1):E75-E84. doi:10.1073/pnas.1614777114
104. Worlikar T, Zhang M, Ganguly A, et al. Impact of Histotripsy on Development of Intrahepatic Metastases in a Rodent Liver Tumor Model. *Cancers (Basel)*. 2022;14(7):1612. doi:10.3390/cancers14071612
105. Lundt J, Allen S, Shi J, Hall TL, Cain CA, Xu Z. Noninvasive, Rapid Ablation of Tissue Volume Using Histotripsy. *Ultrasound Med Biol*. 2017;43(12):2834-2847. doi:10.1016/j.ultrasmedbio.2017.08.006
106. Gerhardson T, Sukovich J, Pandey A, Hall TL, Cain CA, Xu Z. Effect of Frequency and Focal Spacing on Transcranial Histotripsy Clot Liquefaction, Using Electronic Focal Steering. *Ultrasound Med Biol*. 2017;43(10):2302-2317. doi:10.1016/j.ultrasmedbio.2017.06.010

107. Zhang X, Owens G, Cain CA, Gurm HS, Macoskey JE, Xu Z. Histotripsy Thrombolysis on Retracted Clots. *Ultrasound Med Biol*. 2016;42(8):1903-1918. doi:10.1016/j.ultrasmedbio.2016.03.027
108. Haas RLM, Miah AB, LePechoux C, et al. Preoperative radiotherapy for extremity soft tissue sarcoma; past, present and future perspectives on dose fractionation regimens and combined modality strategies. *Radiother Oncol*. 2016;119(1):14-21. doi:10.1016/j.radonc.2015.12.002
109. Seifert JK, Morris DL. World Survey on the Complications of Hepatic and Prostate Cryotherapy. *World J Surg*. 1999;23(2):109-114. doi:10.1007/pl00013173
110. Wah TM, Arrellano RS, Gervais DA, et al. Image-guided Percutaneous Radiofrequency Ablation and Incidence of Post–Radiofrequency Ablation Syndrome: Prospective Survey. *Radiology*. 2005;237(3):1097-1102. doi:https://doi.org/10.1148/radiol.2373042008